INVESTIGATION OF SILVER CATALYST FOR PROPYLENE EPOXIDATION: PROMOTION AND REACTION MECHANISM

by

Marco Antonio Bedolla Pantoja

A thesis submitted to the Faculty of the University of Delaware in partial fulfillment of the requirements for the degree of Honors Bachelor of Chemical Engineering with Distinction.

Spring 2010

INVESTIGATION OF SILVER CATALYST FOR PROPYLENE EPOXIDATION: PROMOTION AND REACTION MECHANISM

by

Marco Antonio Bedolla Pantoja

Approved: _____

Mark A. Barteau, Ph.D.
Professor in charge of thesis on behalf of the Advisory Committee

Approved: _____

Jochen Lauterbach, Ph.D.
Committee member from the Department of Chemical Engineering

Approved: _____

Norbert Mulders, Ph.D.
Committee member from the Board of Senior Thesis Readers

Approved: _____

Alan Fox, Ph.D.
Director, University Honors Program

ACKNOWLEDGMENTS

I wish to thank all of the people that contributed to the success of this publication. First, I would like to thank Dr. Joseph Dellamorte, who taught me everything that there is to know in the lab. The time we spent together in the lab also instilled in us a great sense of comradeship and respect for each other.

I thank my thesis advisor, Dr. Mark Barteu, who gave me the opportunity and freedom to conduct the research that led to this thesis. I admire his patience and determination to his work and his students. Above all, however, I admire his courage for allowing an undergraduate student to manage his research laboratory.

I also would like to thanks my family from whom I have always received unconditional support. Mama, Papa, Javier, Mariana, Alvaro, thank you for your infinite patience even in times when I do not have patience for myself, and thanks for understandings that all these sacrifices have been for a reason. *Gracias, Familia!*

TABLE OF CONTENTS

LIST OF TABLES

LIST OF FIGURES

ABSTRACT

The gas-phase epoxidation of propylene on silver catalysts has been examined. Drawing parallels from the successful catalysts used in ethylene epoxidation, several silver-based catalysts have been tested for propylene epoxidation. However, no catalyst proved to be selective to the desired product, propylene oxide. Cadmium, copper, cesium and rhenium were tested as promoters to silver, but no catalyst achieved more than 5% selectivity to propylene oxide under the conditions tested. When the catalysts were tested at 267 °C with a feed consisting of a gas mixture of propylene, oxygen and nitrogen at volume ratio of 1:1:8, the unpromoted silver catalyst was the least selective. The most selective catalyst was the copper-silver catalyst, which exhibited 4.3% selectivity to propylene oxide. The main limitation to selectivity is the high degree of combustion of propylene to carbon dioxide.

By running the catalysts at different reaction conditions, important conclusions were drawn regarding the the kinetics of the reaction. The conversion of propylene increased as the volume ratio of oxygen to propylene fed to the reactor increased. As the oxygen fed to the reactor was increased with respect to propylene, the conversion of propylene increased but the selectivity to propylene oxide remained nearly constant for all but the rhenium-silver catalyst. For the rhenium-silver catalyst the selectivity decreased as the oxygen to propylene ratio was increased. The reaction order with respect to oxygen for propylene oxidation was deduced from these data. For the silver, cadmium-silver and rhenium-silver catalysts, the reaction order was greater than 1. However, for the cesium-silver and copper-silver catalysts the reaction order with respect to oxygen was 0.4 and 0.5, respectively. The propylene effect of the

activity of the cesium-silver and copper-silver catalysts was also studied. The conversion of propylene decreased as the propylene fed to the reactor was increased with respect to oxygen. These results indicate that oxygen, and not propylene, controls the rate for propylene oxidation. This hypothesis was confirmed by measuring the apparent activation energy for the reaction. For all the catalysts tested the apparent activation energy was 14-17 kcal/mol, in agreement with the energy of oxygen dissociation on silver. Thus, it was concluded that oxygen dissociation is the rate determining step of propylene oxidation.

The decomposition of the desired product, propylene oxide, was also analyzed. Propylene oxide was introduced to an unpromoted silver catalyst that had been previously tested for propylene oxidation. Acetone, acrolein, allyl alcohol and propanal were detected on the effluent stream from the reactor. However, propanal was produced in larger amounts than any other compound regardless of the conditions at which the reaction was run. At 267 °C, for example, the selectivity to propanal was 73 %, to acrolein 14.8 % and for acetone and allyl alcohol 7.0% and 5.2%, respectively. As the reaction temperature was decreased, propanal selectivity increased at about the same rate as acrolein selectivity decreased. The selectivities to acetone and allyl alcohol remained constant. However, further experiments reveal that all of the products from PO decomposition are primary products. By probing this reaction under different conditions, a mechanism of propylene epoxidation has been proposed. The proposed mechanism assumes an oxametallacycle as the crucial intermediate from which acetone, propylene oxide, propanal, acrolein and allyl alcohol are formed. All of these are products of competing reactions of surface oxametallacycles. Acrolein and allyl alcohol are formed through dehydrogenations of the oxametallacycle while

acetone and propanal are formed through 1,2 H-shifts. PO is formed through simple ring closing of the oxametallacycle.

The kinetics and mechanism investigated in this work provides important insights that will help guide the search for a selective catalyst for propylene epoxidation. However, future work needs to address the need to learn more about the relative ease with which the oxametallacycle undergoes ring closing against alternative reactions. This can be accomplished through Density Functional Theory calculations or careful desorption experiments.

Chapter 1

INTRODUCTION

Epoxidation refers to the addition of an oxygen atom to a carbon-carbon double bond to produce a three-atom ring structure called the epoxide (Figure 1.1).

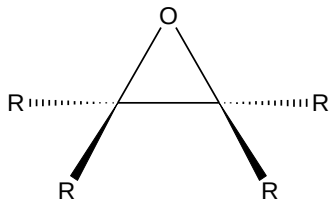

Figure 1.1 The epoxide group

Simple epoxides such as ethylene oxide and propylene oxide have been synthesized since the mid-1800s, but it was not until the 1900s and World War I that their value as chemical intermediates brought about their commercialization [1, 2].Currently, both of these compounds rank among the most widely produced chemicals in the world as measured by their yearly mass production. These epoxides were originally manufactured through the chlorohydrin processes, a homogenous chemical reaction that produces large amounts of brine waste. In 1931, however, it was discovered that silver (Ag) catalyzed the direct oxidation of ethylene into ethylene oxide (Figure 1.2) [1].

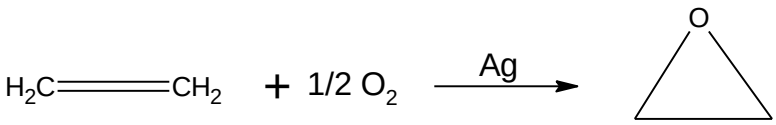

Figure 1.2 Direct epoxidation of ethylene into ethylene oxide using silver

Shortly thereafter, this became the preferred method for ethylene oxide production, even though little was understood regarding the mechanism of the reaction. It was not until the 1990s when Barteau and coworkers were able to identify the crucial reaction intermediate, an oxametallacycle [3, 4]. This discovery, coupled with the successful use of theoretical predictions, led to an understanding of the reaction mechanism, Figure 1.3, and the finding that addition of copper leads to a more active and selective silver catalyst [5, 6, 7].

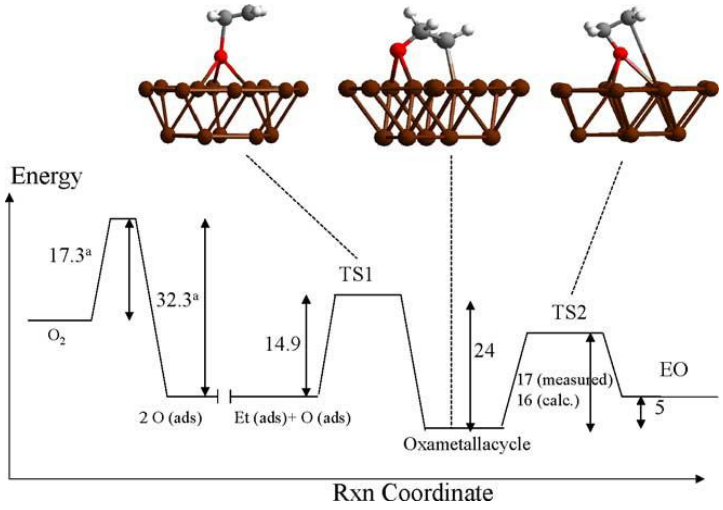

Figure 1.3 Reaction coordinate for epoxidation of ethylene on silver [5]

Nonetheless, these advances have not been easily extended to olefins containing allylic hydrogens, such as propylene. Even though demand for propylene oxide is high due to its use as an intermediate in the manufacture of plastics, fuel additives and urethane foams, etc. production of propylene oxide by direct catalytic oxidation is still not economically viable [8]

Propylene oxide (PO) is currently produced through either the chlorohydrin process or the hydroperoxide process. In the former, epoxidation is carried via the S_N2 elimination of chlorine from the chlorohydrin intermediate $CH_3CH(OH)CH_2Cl$. The reaction generates stoichiometric amounts of calcium chloride ($CaCl_2$), along with other environmentally hazardous byproducts such as 1,2-dichloropropane and some ethers, which create problems with the treatment and disposal of chemical waste. In the organic hydroperoxide method, propylene is reacted with an organic hydroperoxide such as ethyl benzene peroxide or t-butyl peroxide to produce propylene oxide and the corresponding alcohol. Thus, the economic viability of PO production using this method is linked to the market value of the co-products such as 1-phenylethanol or *tert*-butanol [2].

With the goal of replacing current methods for propylene oxide production, several new chemistries have emerged with promising results. Heterogeneous catalysts such as palladium supported on titanium silicalite (TS-1) and gold supported on titanium dioxide (TiO_2) represent some of the most recent developments on propylene epoxidation [9]. However, processes based on these catalysts are economically expensive since they require a supply or in situ generation of peroxides. Silver by itself cannot be used for direct gas-phase propylene epoxidation as is done with ethylene because of the methyl group in propylene.

Previous work suggests that the abstraction of the allylic hydrogen in propylene by adsorbed oxygen leads to combustion and low catalyst selectivity to PO, see Figure 1.4 [10].

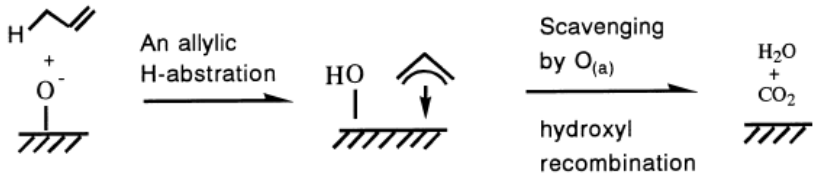

Figure 1.4 Mechanism of propylene combustion on silver [11]

Nonetheless, several reports offer some optimistic results. Gaffney and coworkers, for example, have shown that selective epoxidation of propylene can be achieved with a silver catalyst. Using potassium (K) as a promoter to silver and feeding ethyl chloride (EtCl) and nitric oxide (NO) to the reaction, they obtained propylene conversions of ~10% and PO selectivities of ~50% [12]. Monnier and coworkers also reported selectivities to PO close to 40% by co-feeding butadiene to the reaction, although this strategy resulted in low propylene conversions (<1%) [13].

While these reports show promise improving catalyst selectivity, they raise more questions regarding the underlying chemistry behind propylene epoxidation. As was the case with ethylene epoxidation, a more fundamental understanding of the mechanism of epoxidation is needed. Knowledge of the mechanism of the reaction allows for successful characterization of the relevant steps that affect selectivity toward PO and propylene conversion. This information in turn

will allow for the intelligent design of more selective and active catalysts. It is the goal of this work to help fulfill these roles.

The purpose of this work is two-fold. First, an investigation was carried out to measure the performance of silver catalysts for the epoxidation of propylene, especially those commonly used for ethylene epoxidation. We present data on the reaction orders, activation energies, selectivity and conversion achieved using silver catalysts promoted with other metals such as cadmium, copper, cesium and rhenium. Then we present theoretical results that aim to explain the reaction network involved for the epoxidation of propylene into propylene oxide. In this part, a series of experiments was conducted in order to elucidate propylene oxide formation and loss channels. The purpose of this thesis is to contribute to the mechanistic understanding of the propylene epoxidation, knowledge that will serve in the future for rational catalyst design.

Chapter 2

EXPERIMENTAL METHODS

The experimental approach for the reactor studies based upon successful methods implemented for ethylene epoxidation. The reaction was studied in a plug-flow reactor which used alumina monoliths impregnated with silver as a catalyst. This chapter discusses the methods and equipment set-up utilized in the experiments described in later chapters. The detailed recipe for the preparation of catalysts is provided. The set-up for the reactor and gas chromatograph, used for analysis of the reactor effluent, are discussed along with the pertinent equations for calculation of product selectivities and reactant conversion. The subsequent modification of the reactor to allow for experiments on the decomposition of propylene oxide is also discussed.

2.1 Catalyst Preparation

The preparation of catalysts for propylene epoxidation is well documented from the studies on ethylene epoxidation by Dellamorte [14, 15, 16].The support, an alumina (α-Al_2O_3) monolith, was used because it provided a rigid and self-supporting structure for the catalyst. The foam monoliths made from 99.5% α-Al_2O_3 were provided by Vesuvius Hi-Tech Ceramics. The monoliths were small cylinders with 18 mm diameter and 10 mm length, a porosity of 45 pores per inch (80% porosity) and a surface area of ~0.25 m^2/g [17]. Since the combustion of propylene oxide is a

significant problem for selectivity, the small surface area and porosity of the monolith is required for a short contact time of the products and reactants with the silver (Ag) catalyst.

Prior to catalyst preparation, the monoliths were heated at 700 °C in air for 12 hrs to remove any carbonaceous impurities. Afterward, they were boiled in deionized water for 2 hrs and then dried at 90 °C. Once dried, the catalysts were prepared through wet impregnation of silver nitrate onto the alumina monoliths. The silver nitrate ($AgNO_3$) was dissolved in deionized water, a solution into which the monolith was subsequently immersed. The desired amount of silver nitrate was calculated so that the nominal loading of Ag in all catalysts was between 11-13 wt %. The catalyst was then dried at 90 °C for 6-12 hrs and then calcined at 400 °C in an open air furnace for 12 hrs. Except for cesium (Cs), metal promoters were added to the calcined Ag catalyst via standard solutions containing 1000 µg/mL of the desired metal. Cesium carbonate (Cs_2CO_3), from 1000 µg/mL standard solutions, was added to the monolith along with the silver nitrate solution. A picture of a catalyst is shown in Figure 2.1.

Figure 2.1 Catalyst used for propylene epoxidation: α-Al_2O_3 monolith impregnated with Ag and other metals

After preparation, the catalyst was reduced in a flow of 100 sccm of 20% H_2 in He at 300 °C for an additional 12 hrs. The epoxidation reaction was then initiated by introducing nitrogen and propylene to the reactor at 247 °C, and slowly heating up the catalyst to 267 °C while introducing oxygen. To allow for the reaction to reach steady state, the catalyst was left for 48 hrs under standard reaction conditions. Standard reaction conditions are defined for a catalyst running at 267 °C with an inlet flow of 100 sccm of a mixture of propylene, O_2 and N_2. The volume flow ratio for this mixture is of 1:1:8. Following this treatment, the catalyst was ready to be used in experiments to determine the reaction activation energy, the reaction order of reactants and propylene epoxidation performance.

2.2 Reactor Set-up

The reaction experiments described in this work were carried out using the reactor system shown in Figure 2.2. The catalyst was wrapped with quartz wool and placed inside a 20 mm I.D. quartz tube. The temperature inside the reactor was monitored via a 0.005" diameter bare wire thermocouple strung around the catalyst and connected to an automatic temperature controller. This controller monitored and set the temperature in the tube furnace used to heat the catalyst. The inlet flow to the reactor was provided through mass flow controllers (MFC), each connected to a MFC control box that allowed for the manipulation of the gas flow. Each mass flow controller was properly calibrated for the corresponding gas by measuring the gas flow rate through a bubble meter. The effluent from the reactor was analyzed using a gas chromatograph connected online to a desktop computer. The details of the gas chromatograph are provided below.

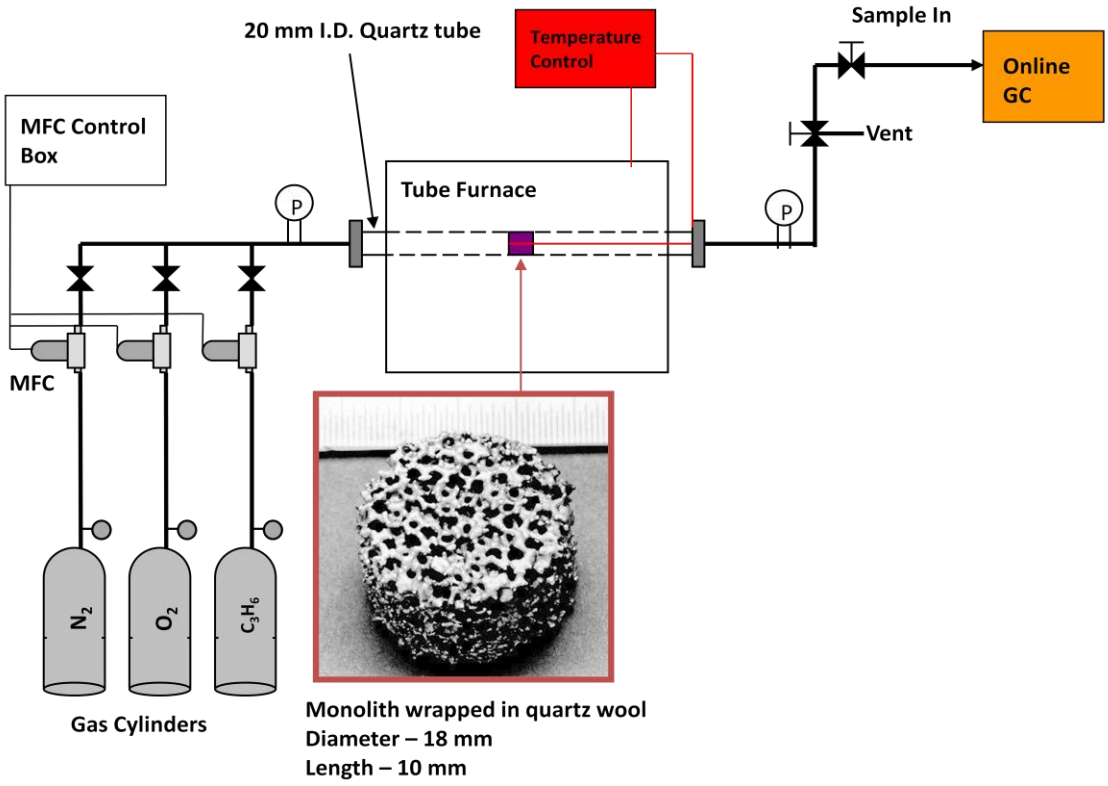

Figure 2.2 Reactor system used in epoxidation experiments [17]

2.3 Gas Chromatograph

The effluent from the reactor was analyzed using a HP6890 gas chromatograph (GC). This apparatus made use of Q Plot capillary columns to separate hydrocarbons, Heysep Q and N to separate CO_2 and 45/60 mesh molecular sieve particles for separation of oxygen and nitrogen. The GC has two detectors, a flame ionization detector (FID) that is used for detection of organics through the Q Plot column, and a thermal conductivity detector (TCD) for the detection of CO_2, O_2 and N_2, mainly. Prior to the experiments mentioned in this work, the gas chromatograph was carefully reconfigured and recalibrated to allow the proper identification of all

chemical species suspected to be present in epoxidation experiments. A temperature ramp was developed, shown in Figure 2.3, to allow proper separation of compounds.

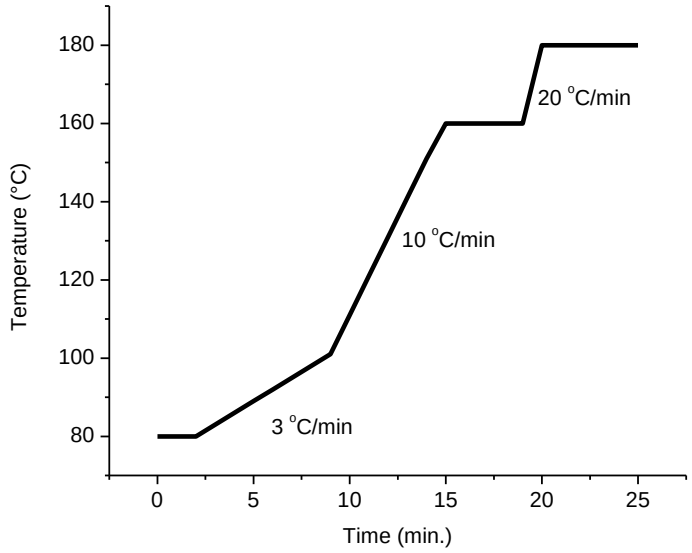

Figure 2.3 Temperature ramp of GC for separation of reactor effluent

The retention time along with the slope for the calibration of the species detected during propylene oxidation are shown in Table 2.1.The calibration was carried out by dosing different concentrations of a given species to the GC and noting the respective response (peak area) in the GC. Note that no FID calibrations were carried for acetone, isopropyl alcohol and allyl alcohol due to lack of resources. The slope of the calibration curve was assumed as 0.05 for these compounds, as this is close to the value obtained for propylene oxide, acrolein and propanal.

For the experiments carried in this work, the conversion and selectivity were calculated on a molar basis according to the following equations:

$$Conversion = \frac{[Propylene]_{TCD}}{[Propylene]_{TCD} + [PO]_{TCD} + {}^{1}/_{3}[CO_2]_{TCD} + [Organics]_{TCD}} x100\%$$

$$Selectivity\ to\ PO = \frac{[PO]_{TCD}}{[PO]_{TCD} + {}^{1}/_{3}[CO_2]_{TCD} + [Organics]_{TCD}} x100\%$$

These equations follow the convention set by Dellamorte and Jankowiak [16, 17].

Table 2.1 Retention times and calibration correlations for the compounds observed during propylene epoxidation

Thermal Conductivity Detector (TCD)	Retention Time [min]	Slope of Linear Correlation
Carbon Dioxide	2.5	0.057
Oxygen	5.3	0.055
Nitrogen	6.2	0.09
Propylene	10.7	0.07
Water	13.7	
Carbon monoxide	15.9	
Propylene oxide	20.8	0.048
Acrolein	22.0	0.053
Propanal	22.4	0.052
Acetone	23.4	
Flame Ionization Detector (FID)		
Propylene	2.5	0.079
Propylene oxide	8.7	0.054
Acrolein	8.9	0.047
Propanal	9.4	0.053
Acetone	10.3	
Isopropyl Alcohol	11.7	
Allyl Alcohol	12.5	

Chapter 3

PROPYLENE EPOXIDATION: KINETICS AND CATALYST PERFORMANCE

In this chapter, a discussion is presented of the direct epoxidation of propylene into propylene oxide. The goal of these investigations was to draw parallels to the epoxidation of ethylene, a successful process currently practiced commercially. Thus, the catalysts and methods commonly used for ethylene epoxidation were extended to the epoxidation of propylene. The effectiveness of silver and metal-silver promoted catalyst was investigated for propylene epoxidation and an elementary analysis of the kinetics is presented. The conversion of propylene and the selectivity to propylene oxide was studied for varying reaction conditions and for different metal promoters. The present results serve to elucidate of important mechanistic details for the epoxidation of propylene, which in turn will allow for the design of highly selective catalysts for this reaction.

3.1 Effect of Metal Promoters on the Selectivity to Propylene Oxide

Experiments on propylene epoxidation were carried using catalysts containing silver (Ag) and silver promoted with cadmium (Cd), cesium (Cs), copper (Cu) or rhenium (Re). These metals were chosen since they have been shown to increase the selectivity to ethylene oxide in the oxidation of ethylene on Ag [6, 16, 18, 19, 20]. With the assumption that similar improvements would be observed for propylene epoxidation, the concentrations of metal promoters in the Ag catalysts,

shown in Table 3.1, were chosen because, according to Dellamorte, they gave optimal selectivity to ethylene oxide [16].

Table 3.1 Metals added to silver catalyst as selectivity promoters for propylene epoxidation. Catalysts contain 11-13 wt % of silver on α-Al_2O_3

Promoter	Concentration (ppm)
Cd	80
Cs	500
Cu	300
Re	25

All catalysts were prepared in the same manner and tested at similar reaction conditions as described in the methods section of this work. Thus, for convenience sake, they will be simply referred to by the convention "promoter-Ag". For example, the catalysts impregnated with 80 ppm Cd will be referred to as Cd-Ag.

Running at standard reaction conditions, the products observed varied depending on the catalyst used. Nonetheless, typical products included propylene oxide, acrolein, propanal and acetone. Figure 3.1 offers a sample GC spectrum for the observed products and their retention time in the GC. It is noted, also, that the catalysts tested from different batches presented minor variations in selectivity to products and conversion of propylene. The results presented below are taken from a representative sample of the catalysts tested.

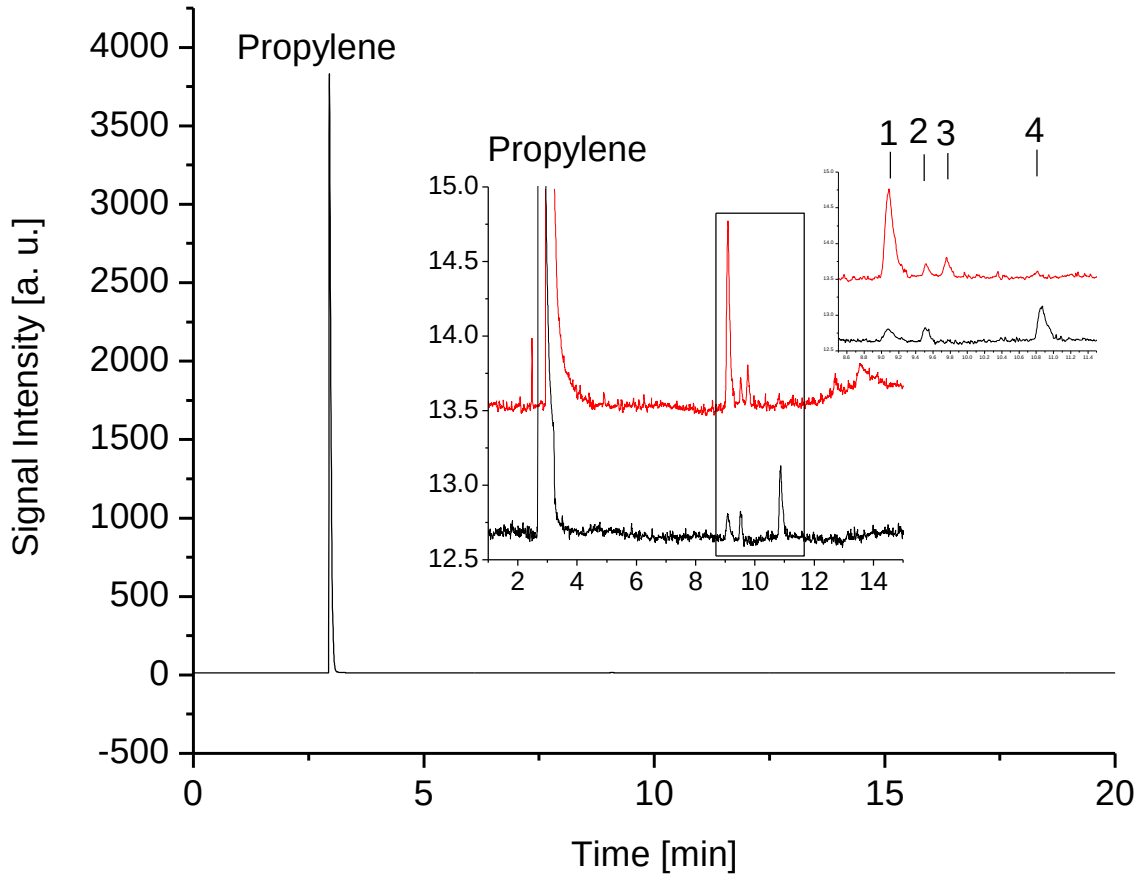

Figure 3.1 Sample GC (FID) spectra for propylene epoxidation. The inset shows the products typically observed during the epoxidation experiments: 1) propylene oxide, 2) acrolein and 3) propanal and 4) acetone

Despite the variation of the selectivity from catalyst to catalyst, the pattern for propylene oxidation remained the same regardless of the catalyst under consideration. Combustion of propylene to carbon dioxide (CO_2) was the dominant reaction for all catalysts tested. As can be seen in Table 3.2, which shows the product

distribution for each catalyst, the selectivity of the reaction to CO_2 was greater than 90% for all but the Re-Ag catalyst. Meanwhile, the selectivity to propylene oxide and the conversion of propylene was never greater than 5%.

Table 3.2 Reaction products for catalysts used in epoxidation. Reaction at standard conditions

Catalyst	Propylene Conversion (%)	Selectivity to :				
		Carbon Dioxide	Propylene Oxide	Acrolein	Acetone	Propanal
Ag	1.4	98.5	~0.0*	1.5	0.0	~0.0*
Cd-Ag	3.5	99.0	0.9	0.1	~0.0*	0.0
Cs-Ag	3.4	98.2	1.6	0.2	~0.0*	~0.0*
Cu-Ag	4.6	95.6	4.3	0.1	0.0	0.0
Re-Ag	0.2	87.4	3.2	1.6	7.8	0.0

*Peaks too small to quantify but non-zero

The unpromoted Ag catalyst was essentially unselective for propylene oxide, producing acrolein instead. This catalyst also exhibited the lowest activity, aside from the Re-Ag catalysts, with a 1.4% overall conversion of propylene.

The Re-Ag catalyst had the lowest conversion of the catalysts tested. This catalyst produced a relatively high amount of PO, as measured by the selectivity of 3.2%, however the selectivity to acetone using this catalyst was even higher than the selectivity to PO (7.8%).

The Cs-Ag and the Cd-Ag catalysts gave about the same conversion of propylene (3.5%). Nonetheless, Cd-Ag exhibited the lowest selectivity to PO (0.9%) of all the promoted catalysts. The Cs-Ag catalyst, in contrast, exhibited a much higher selectivity to PO at 1.6%, though still inferior to that from the Cu-Ag and Re-Ag catalysts. Both the Cd-Ag and the Cs-Ag catalysts also produced other side products such as acetone and propanal.

The Cu-Ag catalyst showed the greatest activity of all catalysts tested at 4.6 % conversion and 4.3 % selectivity to PO. This result is consistent with ethylene epoxidation, in which a Cu-Ag catalyst exhibited increased activity and selectivity as compared to unpromoted Ag catalysts [6]. From this analysis alone, it can be concluded that Cs-Ag and Cu-Ag catalysts give the best performance for propylene epoxidation. However, the high production of carbon dioxide as compared to PO is still a major hurdle to the selective epoxidation of propylene for all the Ag and Ag-based catalysts used.

3.2 Oxygen Dependence of the Activity of the Ag-based Catalysts for Propylene Oxidation

Moving away from the standard reaction conditions, the effect of the partial pressure of the reactants on the reaction can be characterized. For catalysts running under oxidizing conditions (excess oxygen, O_2, in the feed), conversion of propylene depended in oxygen flow rate. For these experiments, the flow rate of propylene remained at 10 sccm while the oxygen flow was increased. Nitrogen flow was adjusted accordingly to keep the total flow at 100 sccm. As shown in Figure 3.2, the conversion of propylene increased somewhat as the volume ratio of O_2 to propylene was increased in the feed for the different catalysts. The rate of change of the conversion varied, though, with the catalyst tested. For the Cd-Ag catalyst, for example, the conversion increased from 3.5% to over 11% as the O_2 to propylene volume flow ratio was increased from 1 to 3. A similar trend was observed for Ag. In contrast, the change in conversion for the Re-Ag catalyst was negligible, going from a low of 0.2% to 0.7% while the O_2/propylene ratio was increased from 1 to 4.5. The change in propylene conversion was less dramatic for the Cs-Ag and Cu-Ag catalysts,

for which the rate of change of propylene conversion with respect to ratio of reactants was intermediate between those exhibited by the Cd-Ag and the Re-Ag catalysts.

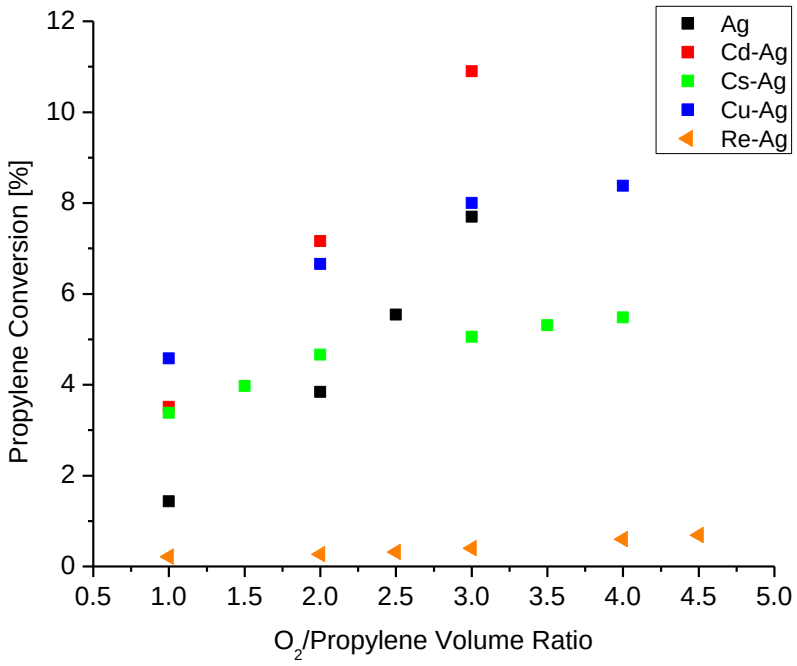

Figure 3.2 Effect of O_2/propylene volume ratio on the conversion of propylene. Catalysts running at 267 °C and 10 sccm propylene.

Despite the increases in conversion for all catalysts, the selectivity to PO remained fairly constant as the O_2/propylene ratio was changed. Figure 3.3 shows the data for the variation of selectivity to PO as the ratio of reactants was changed. Of the catalysts tested, only the Re-Ag exhibits a decrease in the selectivity of PO. All the others show small, if any, increase in PO selectivity even as the conversion increased at a higher rate. The most dramatic example is given by the Cd-Ag catalyst, for which

the PO selectivity remained at ~1% while the conversion increased from 3.5% to over 11% as the ratio of the reactants in increased. The behavior of the Re-Ag and the Cd-Ag catalysts can be explained by the direct combustion of propylene shown in Figure 1.4. In this scheme, the allylic hydrogen of propylene is extracted by oxygen adsorbed on the surface. The following explanation is proposed for the behavior of conversion and selectivity shown in Figures 3.2 and 3.3. On the Ag, Cd-Ag and Re-Ag catalysts, the properties of the surface are such that the direct oxidation increases at a faster pace than oxametallacycle formation (which leads to PO) as O_2 is increased relative to propylene. For the other catalysts, Cs-Ag and Cu-Ag, the rate of propylene combustion and oxametallacycle formation increase roughly at the same pace, which explains the modest selectivity gains accompanying to the conversion increase as the ratio of reactants was increased.

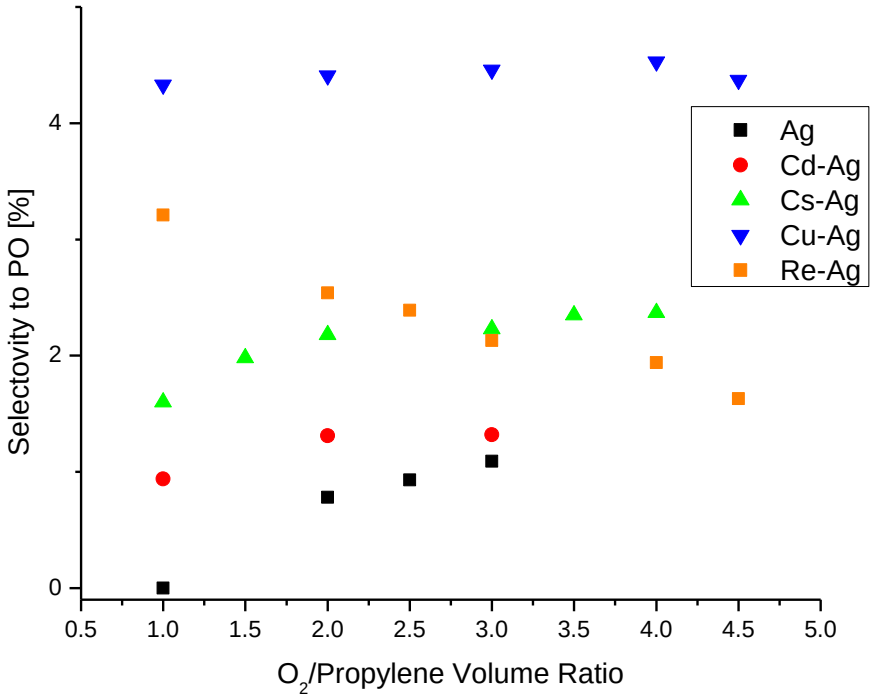

Figure 3.3 Effect of O_2/propylene volume ratio on the selectivity to propylene oxide, PO. Catalysts running at 267 °C and 10 sccm propylene

The effect of oxygen on the reaction can be further quantified through the reaction order with respect to oxygen. For this purpose, the following reaction rate equation was assumed:

$$-r_p = kP_p^{\alpha} P_{O_2}^{\beta} \tag{3.1}$$

The rate of propylene consumption is represented by $-r_p$, k is the temperature dependent rate constant, $P_p$and $P_{O_2}$are the partial pressures of propylene and oxygen, respectively. The corresponding reaction orders are $\alpha$and β. The rate of

the reaction is based on the conversion of propylene according to the following equation:

$$-r_p = \frac{(InitialMolarFlowRateofPropylene) * (PropyleneConversion)}{WeightofCatalyst}$$

Plotting $\ln(-r_p)$ vs. $\ln(P_i)$, where i is either p or O_2, the reaction order for the reactants can be determined. An example of this graph is shown in Figure 3.4

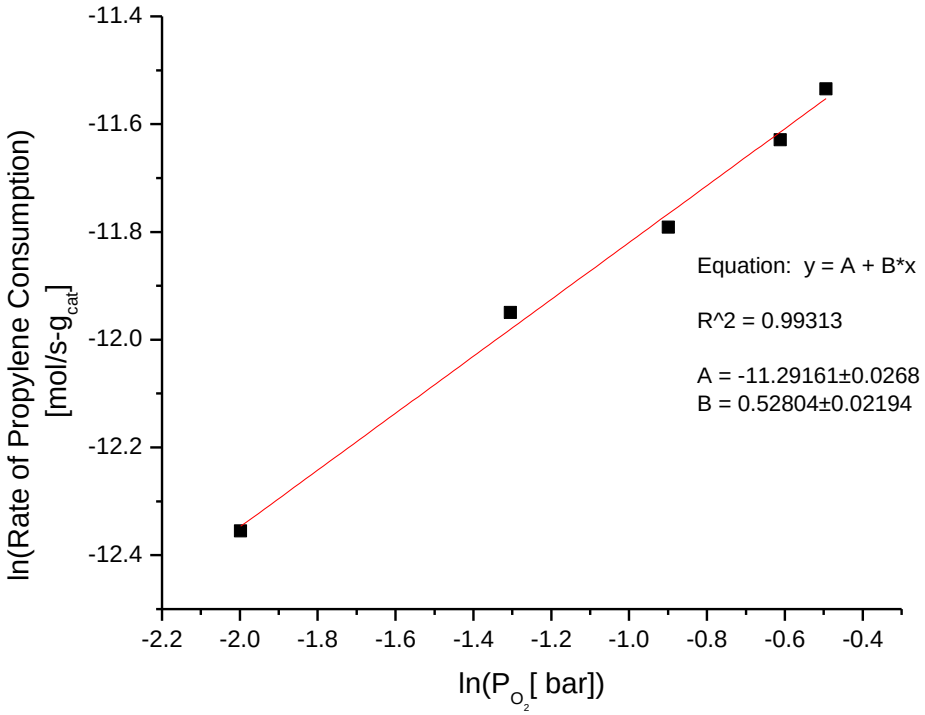

Figure 3.4 Sample plot for the determination of oxygen reaction order. In this example, a Cu-Ag catalyst, the slope of the line, a = 0.5, gives the apparent reaction order with respect to oxygen

The measured reaction order for oxygen on the catalysts tested in shown in Table 3.2. Most of the measured reaction orders were greater than one, which is explained by the high amount of propylene combustion. Only the Cs-Ag and the Cu-Ag catalysts exhibited a much lower oxygen reaction order.

Table 3.2 Oxygen reaction order for propylene epoxidation in different catalysts

Catalyst	Reaction order with respect to oxygen
Ag	1.5
Cd-Ag	1.0
Cs-Ag	0.4
Cu-Ag	0.5
Re-Ag	1.2

3.3 Propylene Dependence of the Activity of Ag-based Catalysts for Propylene Oxidation

The effects of reducing conditions on the reaction were also studied, albeit only for the Cu-Ag and the Cs-Ag catalysts, which were deemed the most interesting based on their conversion of propylene, propylene oxide selectivity, and their behavior under oxidizing conditions. In this set of experiments, the oxygen flow to the reactor was kept constant at 10 sccm while the propylene flow was increased. The nitrogen flow was adjusted accordingly to maintain the total flow rate of the gas mixture at 100 sccm. Figure 3.5 shows the propylene conversion data plotted against the O_2/propylene volume ratio, consistent with the previous figures. As expected from an extrapolation of Figure 3.2 for Cu-Ag and Cs-Ag, the propylene conversion increased as the O_2/Propylene ratio decreased.

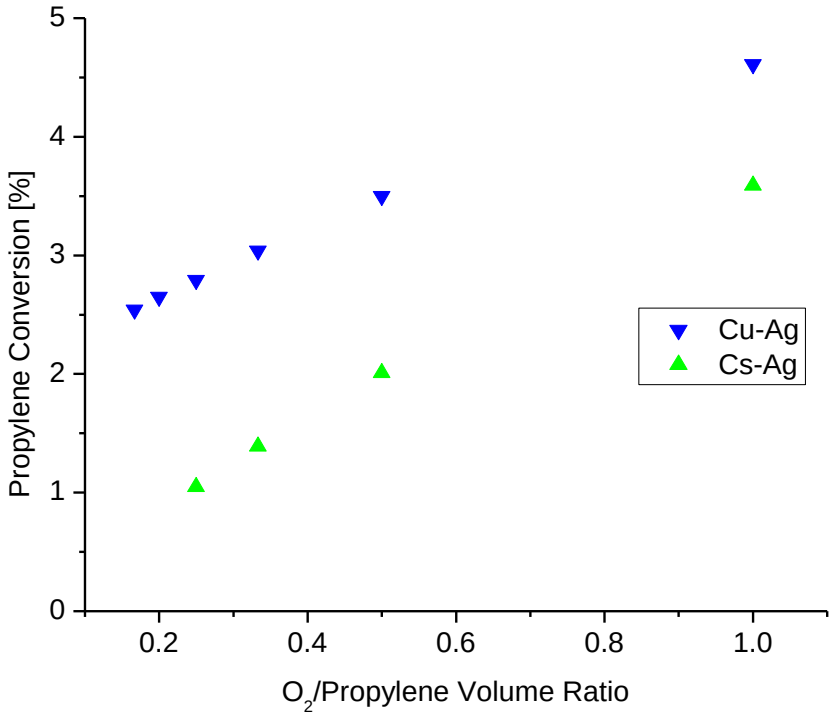

Figure 3.5 Effect of O_2/propylene volume ratio on the conversion of propylene. Catalysts running at 267 °C and 10 sccm oxygen while flow of propylene was increased

These results indicate that it is oxygen, and not propylene, which controls the rate for the reaction under consideration, mainly combustion of propylene to CO_2. As the oxygen feed pressure is increased relative to propylene the oxygen surface coverage increases, which leads to higher reaction rates and thus increased conversion. Larger propylene feeds relative to oxygen reduce the oxygen concentration on the working catalyst.

The effects of reducing catalyst conditions on the selectivity to propylene oxide were less clear than under oxidizing conditions. For one thing, the amount of

acrolein produced increased at a faster rate than the amount of PO produced. A sample GC spectrum for the observed effect can be seen in Figure 3.6 for a Cs-Ag catalyst. This effect, which was not observed for the data collected for Figures 3.2 and 3.3, can be explained only if the acrolein and the PO have different reaction pathways for their formation. Lie and Friend report that on Au(111), formation of acrolein through hydrogen activation in propylene competes with the formation of a stable oxametallacycle and subsequent production of PO [21]. By extrapolating their conclusion to the Ag based catalysts used in this work, it then becomes clear that an increase in propylene partial pressure yields a larger increase in acrolein formation than in PO formation.

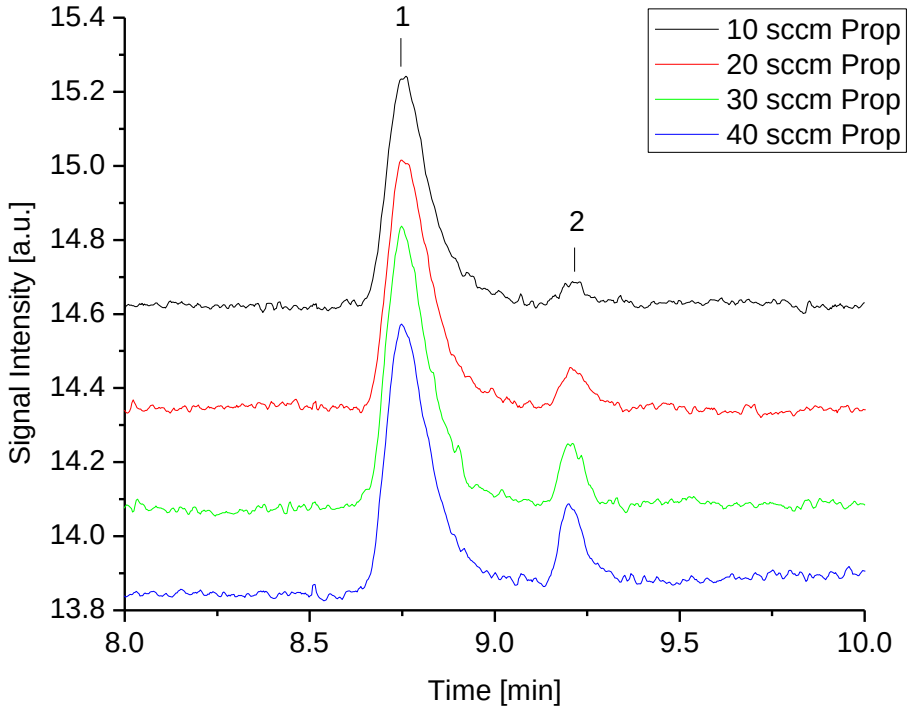

Figure 3.6 Increased acrolein production observed when volume flow of propylene to the reactor was increased. The peaks in the graph are 1) propylene oxide and 2) acrolein. Cs-Ag running at 267 °C and 10 sccm oxygen while flow of propylene is increased

A comparison of the selectivity to PO and to acrolein for the Cu-Ag and Cs-Ag catalysts is shown in Table 3.3. While the PO selectivity remained fairly constant as the propylene is increased, the acrolein selectivity keeps increased. This effect was similar for both catalysts, although the Cu-Ag exhibits twice the selectivity towards both products as the Cs-Ag catalyst.

Table 3.3 Comparison of the selectivities to PO and acrolein of Cu-Ag and Cs-Ag catalysts under reducing conditions

O_2/Prop Ratio	Selectivity (%):			
	PO		Acrolein	
	Cu-Ag	Cs-Ag	Cu-Ag	Cs-Ag
1.00	4.30	1.67	0.00	0.00
0.50	4.26	1.78	0.32	0.19
0.33	4.24	1.87	0.45	0.29
0.25	4.18	1.85	0.60	0.38
0.20	4.15	-	0.76	-
0.17	4.02	-	0.87	-

The reaction order of propylene cannot be quantified as easily as was the case for oxygen. If the data for the propylene partial pressure and the reaction rate is plotted, as was done for Figure 3.4, the resulting graph is not linear. As can be seen in Figure 3.7, the nonlinearity in the data is strong enough so that it cannot be fitted to a line if the model in Equation 3.1 is assumed.

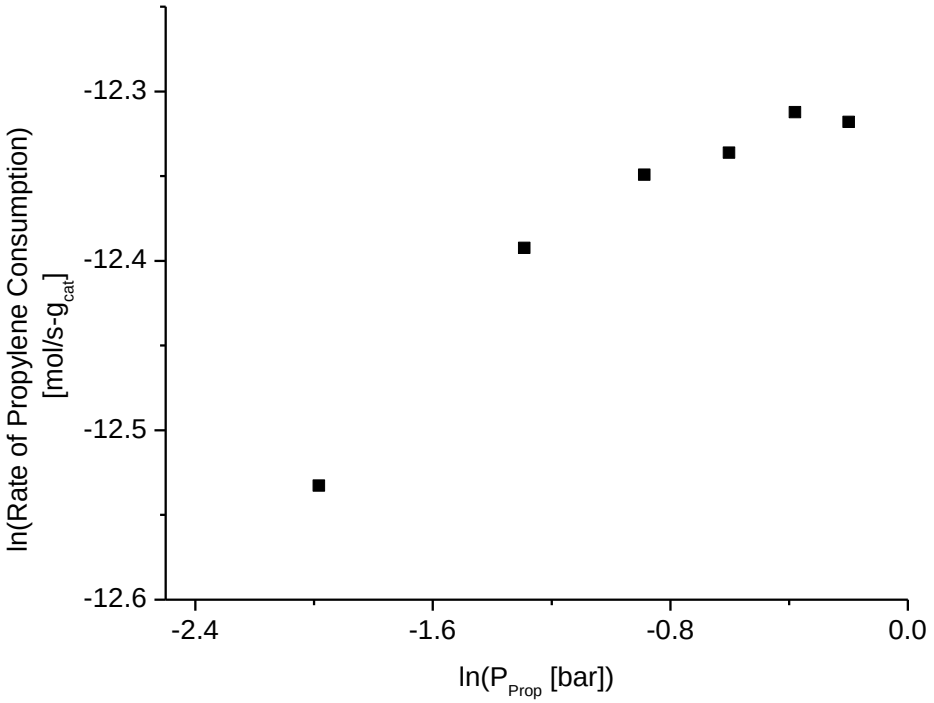

Figure 3.7 Sample plot for the determination of oxygen reaction order for a Cu-Ag catalyst.

However, if a Langmuir-Hinshelwood model is assumed, the data fits the model better than in Figure 3.7. To introduce the required adsorption term in the Langmuir model, Equation 3.1 has to be modified as follows:

$$-r_p = k\left(\frac{AP_p}{1+BP_p}\right)P_{O_2}^{\beta}$$

A and B are constants. By taking the inverse of the reaction rate, it is easily shown the rate expression is linearized by plotting the data as $1/-r_p$ vs. $1/P_p$. The validity of this model for the data at hand is confirmed by improved linearity of

the plot as shown in Figure 3.8 and Table 3.4. Table 3.4 shown the linear-fit parameters from the fits (red-lines) of Figure 3.8

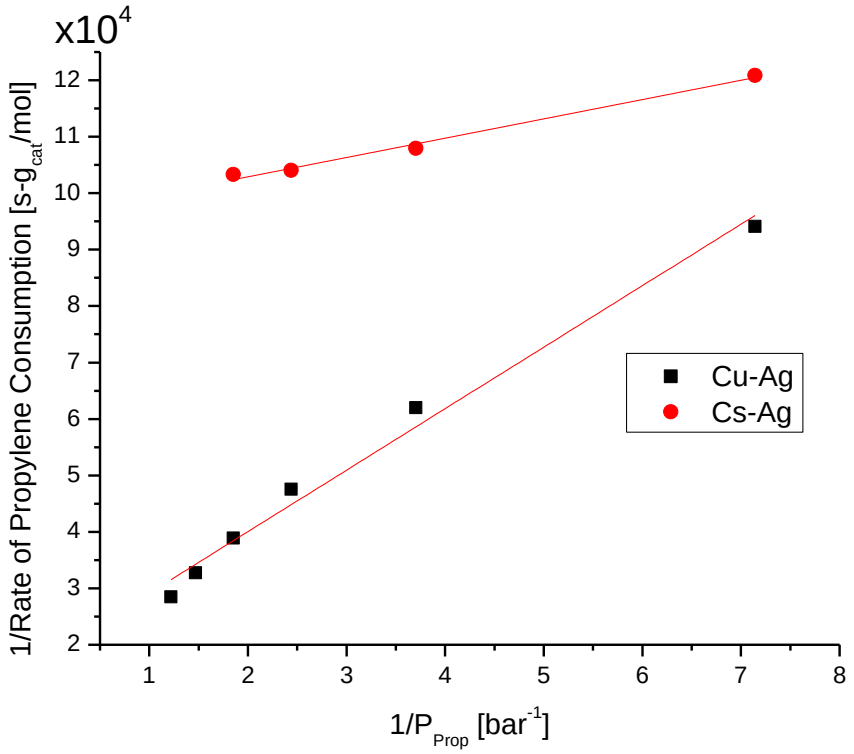

Figure 3.8 Langmuir plot for propylene partial pressure in the reactor

Table 3.4 Linear-fit parameters for data shown in Figure 3.8. Model y = y_0 + b*x

Cs-Ag	
R^2	0.987
$y_0/10^4$	9.6±0.1
$b/10^4$	0.3±0.02

Cu-Ag	
R^2	0.985
$y_0/10^4$	1.8±0.2
$b/10^4$	1.1±0.1

3.4 Apparent Activation Energy for Propylene Oxidation

The apparent activation energy for propylene oxidation with different catalysts was also measured. This experiment was performed by changing the temperature of the reactor while maintaining other conditions constant. In this case, it is assumed that the reaction rate follows Arrhenius behavior with respect to the temperature of the reaction. Thus, in the rate equation assumed above, Equation 3.1, the reaction constant k is given by the following expression:

$$k = Aexp\left(-\frac{E}{RT}\right)$$

The apparent activation energy is E, R is the ideal gas constant and T is the reactor temperature in Kelvin. Therefore, plotting $\ln(-r_p)$ vs. 1/ RT, the data can be fit to a linear equation, if the reaction exhibits Arrhenius behavior, with slope –E, the apparent activation energy of the reaction. An example of the Arrhenius plot constructed from the data for epoxidation as a function of temperature is shown in Figure 3.9.

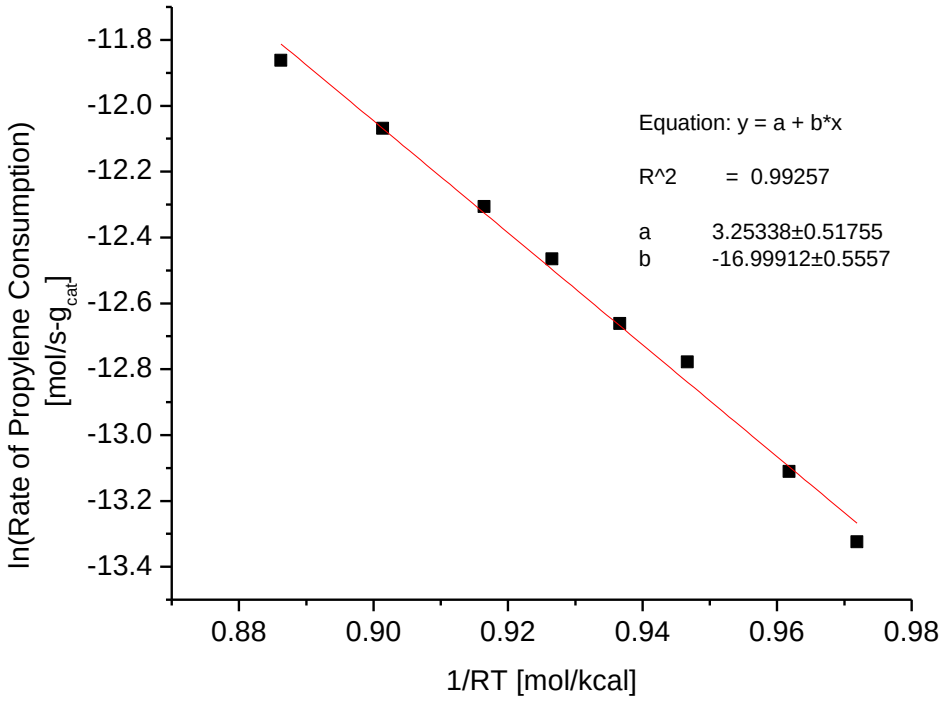

Figure 3.9 Sample plot for the determination of apparent activation energy of propylene oxidation. Cu-Ag catalyst running with 80 sccm N_2, 10 sccm O_2 and 10 sccm propylene. The slope of the line indicates an activation energy of 17 kcal/mol

The apparent activation energies for propylene oxidation on the catalysts studied are shown in Table 3.5. Except for the measured energy on Ag, all other activation energies fall between 14-17 kcal/mol. These results compared well to the energy barrier for dissociation of oxygen on silver, which Norskov et al. calculated to be ~17 kcal/mol [22].

Table 3.5 Measured Activation energies for propylene oxidation on several catalysts

Catalyst	Activation Energy [kcal/mol]
Ag	22.1
Cd-Ag	15.8
Cs-Ag	15.3
Cu-Ag	17.0
Re-Ag	14.9

Since the measured apparent activation energy is similar to that of the oxygen dissociation on silver, it can be presumed that, at least for these catalysts, the dissociation of oxygen on the silver is the rate limiting step under the measured conditions.

Chapter 4

THE MECHANISM OF PROPYLENE EPOXIDATION

In this chapter, a discussion is presented of the decomposition of propylene oxide on silver catalysts. A thorough analysis of this reaction was performed. The effects of temperature, oxygen concentration and flow rate of propylene oxide on the reaction were carefully investigated. The results, along with a discussion of the consequences for the reaction mechanism, are presented in this section.

The purpose of investigating the decomposition of propylene oxide on silver is twofold. First, by observing the products of propylene oxide decomposition under different conditions, some insight can be gained about the mechanism of propylene epoxidation itself. Based on the data presented in this chapter, and assuming an oxametallacycle intermediate, a mechanism for the epoxidation of propylene has been proposed. Knowledge of the details of the mechanism for epoxidation will help guide future work on the design of selective catalysts for the production of propylene oxide. Also, by studying the decomposition of the epoxidation products on silver, their stability can be analyzed. This information reveals further constraints on the development of selective catalysts.

4.1 The Decomposition of Propylene Oxide on Silver

The experiments on the decomposition of propylene oxide, PO, on silver catalysts were guided by the need to explain the variety of the chemical species observed during propylene oxidation. As was shown in Figure 3.1, acrolein, propanal and acetone are observed along with PO and CO_2 during some oxidation experiments. Following the example of Linic and Barteau of the discovery of the reaction pathway for ethylene epoxidation, propylene oxide was fed to an α-Al_2O_3 supported silver catalyst in order to learn about the mechanism of epoxidation [23]. In the experiments described in this section, the catalysts used for the decomposition were first allowed to reach steady state for propylene oxidation. The catalysts were then purged with nitrogen for several hours to remove any propylene or oxygen, after which a stream of 1% PO in nitrogen was introduced into the reactor operating at 267 °C. After steady state was achieved for the decomposition reaction, defined as the point where the conversion of PO and selectivity of the products achieved a stable value, the effects of temperature, oxygen concentration and flow rate on PO decomposition were studied.

Almost all of the products observed during the decomposition experiments were also products of the epoxidation reaction. Figure 4.1 presents a sample GC spectrum for the observed products of PO decomposition, which include acrolein, propanal, acetone and allyl alcohol. In this experiment, CO_2 was not observed, which makes sense since no oxygen was available on the catalyst to attack any of the reaction products. The alcohol is the only product that was not observed during the oxidation experiments.

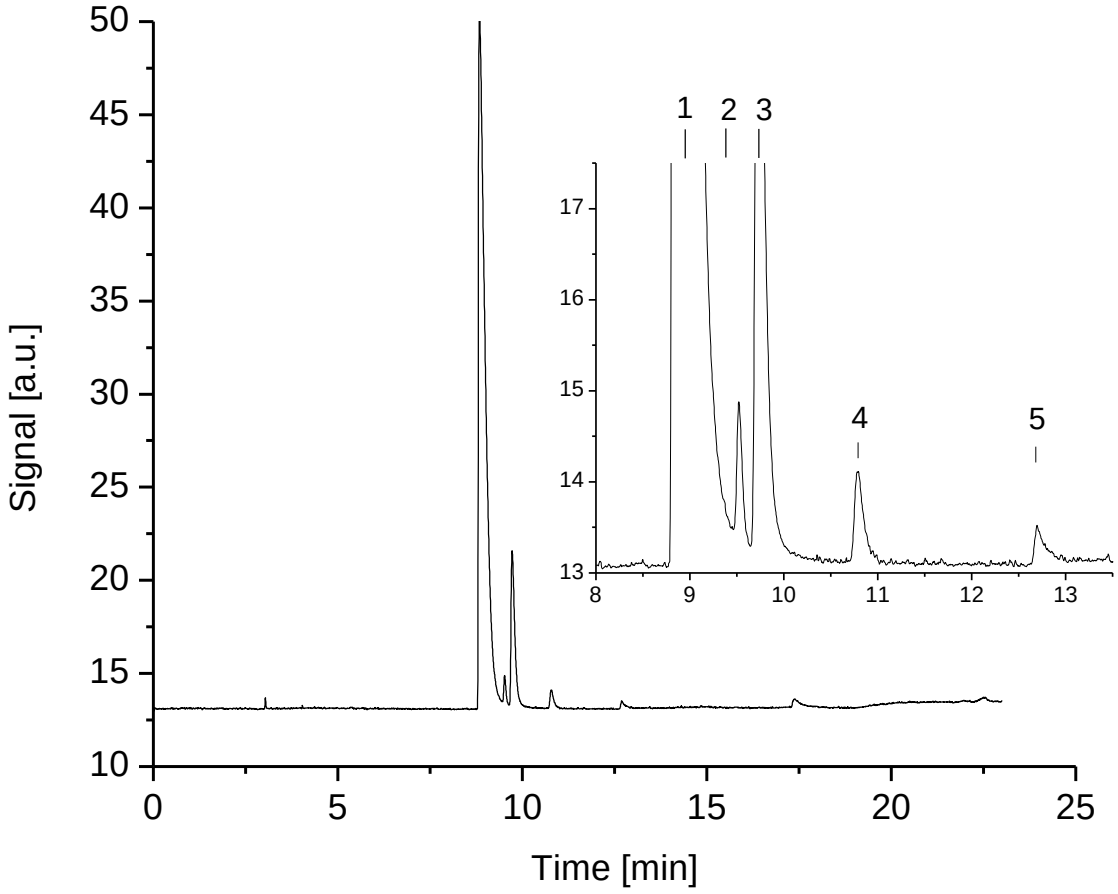

Figure 4.1 Sample GC (FID) spectra for decomposition of propylene oxide on silver. The inset shows the products observed during the decomposition experiments, namely 1) propylene oxide, 2) acrolein and 3) propanal, 4) acetone and 5) allyl alcohol.

For reference, the chemical structures of the compounds under consideration are presented in Figure 4.2. Note that of the observed species, propylene oxide, propanal, acetone and allyl alcohol are isomers. Acrolein, having two hydrogen

atoms less than the other species, is the only non-isomeric product that was observed in the decomposition experiments.

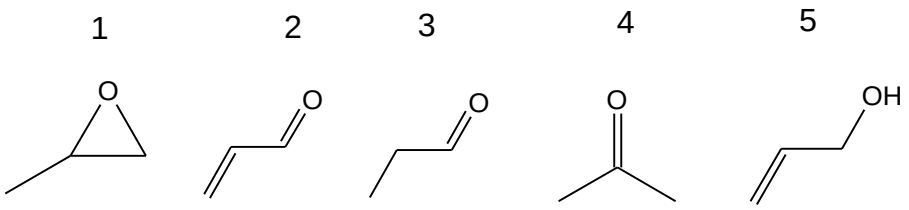

Figure 4.2 Structures of compounds under consideration: 1) propylene oxide, 2) acrolein and 3) propanal, 4) acetone and 5) allyl alcohol

The formation of acetone, allyl alcohol and propanal from propylene oxide can be rationalized from a thermodynamic analysis of these isomeric compounds. Propylene oxide, having a highly strained three-member ring, is expected to be less stable thermodynamically and thus more reactive. In contrast, acetone has a carbonyl group in the keto position, which renders this molecule particularly stable in comparison to the rest. In Table 4.1, the standard heats of formation $\Delta H_f°$, of these compounds are presented. A more negative heat of formation indicates that the molecule under consideration is thermodynamically more stable. As predicted from structural considerations, acetone, with a $\Delta H_f°$ of -51.9 kcal/mol, is the most stable of all while propylene oxide, $\Delta H_f°$ of -22.4 kcal/mol, is the least stable. Thus, it can be expected that given the necessary conditions, propylene oxide will isomerizes into a more stable configuration, and this occurs on the surface of the silver. Nonetheless, propanal is produced in greater amounts than any other product in the isomerization of propylene oxide, even though acetone is clearly a more stable isomer. It can be

hypothesized that this might be due to higher activation barrier for formation of acetone as compared to propanal formation. However, more precise experiments are required before making any conclusions.

Table 4.1 Thermodynamic properties of isomeric products of epoxidation [24]

	Heat of Formation, $\Delta H_f°$ [kcal/mol]	Relative Stability, $\Delta H_f° - \Delta H_f°(PO)$ [kcal/mol]
Propylene oxide	-22.4	0
Acetone	-51.9	-29.5
Allyl alcohol	-29.5	-7.1
Propanal	-44.4	-22

Note that for the data analysis of the subsequent experiments presented in this work, there was a small overlap in the peaks for PO, acrolein and propanal, as shown in Figure 4.1. The integration of the peak areas, however, was carefully performed manually in order to minimize any error from peak overlap.

4.1.1 Temperature Dependence of the Decomposition of Propylene Oxide

The decomposition of PO was studied at different temperatures. In this experiment, PO was fed at 0.5 sccm in a 50 sccm stream of nitrogen to the catalyst and the temperature of the reactor was varied. The behavior of the PO conversion at different temperatures can be observed in Figure 4.3.

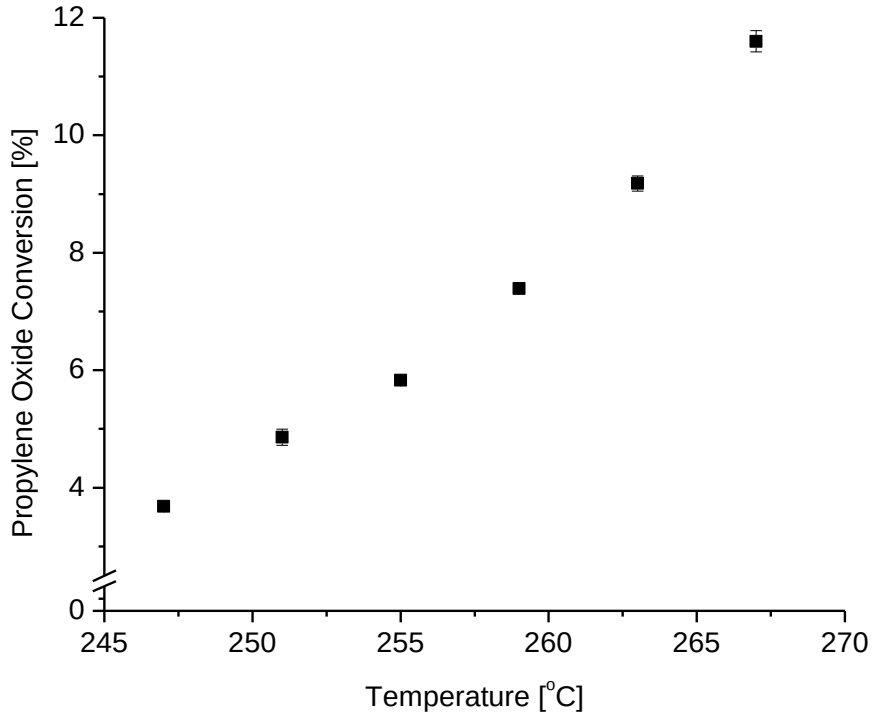

Figure 4.3 Propylene oxide decomposition on Ag at different temperatures

At 267 °C, the conversion of propylene oxide is 11.7% and it appears to change exponentially with temperature. Based on this data, the activation energy for this reaction can be obtained. As was shown in Chapter 3 for epoxidation, the activation energy was calculated by fitting the reaction rate data to an Arrhenius model. The reaction rate is calculated according to the equation below:

$$-r = \frac{(InitialMolarFlowRateofPO) * (POConversion)}{WeightofCatalyst}$$

The Arrhenius plot for the decomposition of PO is shown in Figure 4.4, which shows that the Arrhenius model fits the data quite well. The activation energy

for PO decomposition, given by the slope of the equation, is 31.7 kcal/mol. Note that this value is significantly higher than the apparent activation energy measured for propylene epoxidation, which is ~22 kcal/mol on silver and ~14-17 kcal/mol for other catalysts.

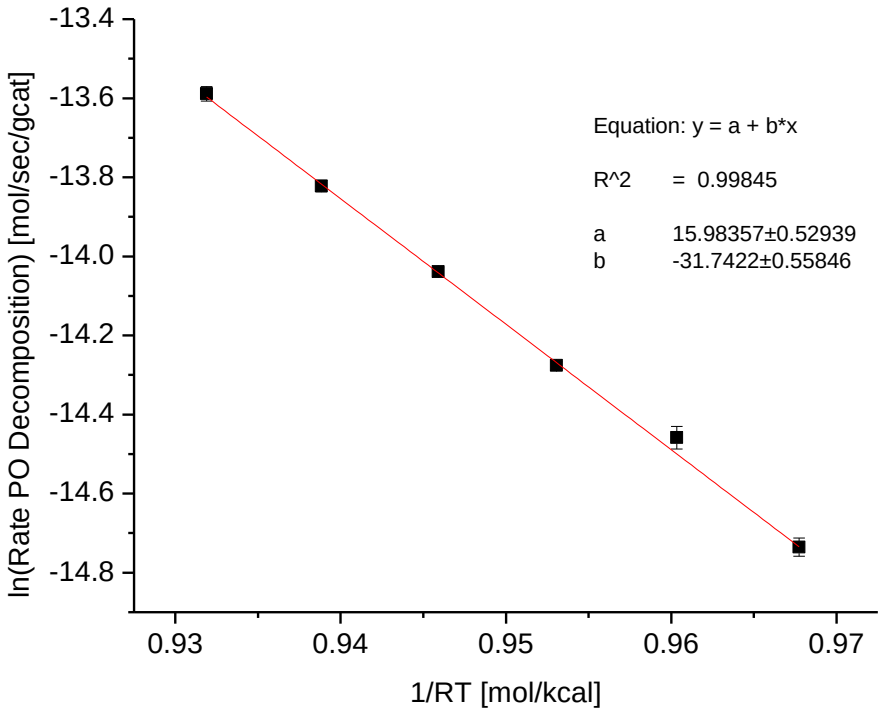

Figure 4.4 Arrhenius plot for the decomposition of propylene oxide on silver. Slope of the linear-fit model gives the activation energy of the reaction, E_a = 31.7 kcal/mol

This value of 31.7 kcal/mol is very similar to the value calculated by Lei et al. for the barrier for oxametallacycle formation from adsorbed propylene oxide.

Using Density Functional Theory calculations, they reported that the energy barrier in going from the adsorbed propylene oxide in the surface to the oxametallacycle formation, the opposite of epoxidation, is 29.1 kcal/mol [25]. This result suggests that formation of the oxametallacycle from adsorbed PO may be the rate limiting step for PO decomposition.

Reaction of propylene oxide on silver yielded mostly propanal. At 247 °C, the selectivity towards propanal was almost 80 %, but as the temperature of the reactor was increased this value rapidly decreased. As can be seen in Figure 4.5, at 11.7% conversion of PO, which corresponds to 267 °C, the selectivity towards propanal decreased to 73 %. At the same time, the selectivity towards acrolein went from 5.8% to 14.8%, an increase that is similar to the decrease in propanal selectivity. These results suggest that propanal and acrolein are produced by competing reactions of a common intermediate. The alternative explanation, that acrolein is formed by reaction of propanal, is refuted through an experiment shown later in this section. Moreover, it can also be reasoned that the high stability of the propanal molecule may prove it difficult for dehydrogenation to occur.

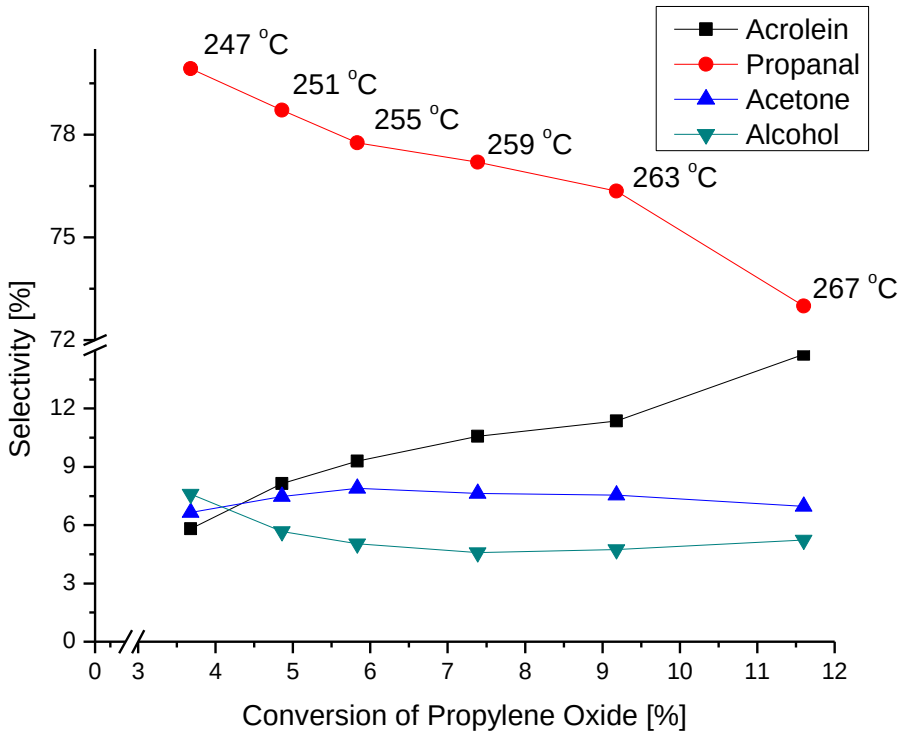

Figure 4.5 Selectivity to various products from propylene oxide decomposition on silver

While the selectivity to acetone and allyl alcohol remains fairly constant as the conversion of propylene oxide changes, the selectivity to acrolein and propanal change in such a way that the lines that are traced on the graph are mirror images of each other. Since it is speculated that propanal and acrolein are produced from competing reactions, the data in Figure 4.5 indicate that one path has a higher activation energy than the other. If an oxametallacycle is assumed as the intermediate by which PO reacts on the surface of the catalyst, then the formation of propanal will proceed through a 1, 2 H-shift of the oxametallacycle. Acrolein formation must go

through a similar path, but on top of that, dehydrogenation must occur at some point. The path to acrolein formation must have higher activation energy than the one leading to formation of the other products; this explains the increase in selectivity to acrolein as the temperature in the catalyst is increased. The hypothesis that propanal and acrolein proceed from competing reaction pathways is further explored by experiments varying the residence time of PO in the reactor.

4.1.2 Exploration of Acrolein Formation from PO Decomposition

The experiments described in this section were carried out by changing the flow rate, and thus the residence time, of propylene oxide to the reactor while maintaining the silver catalyst at constant temperature, 267 °C. Due to equipment limitations, the range for changing the reactant flow rate was fairly limited. The PO flow was increased linearly from 0.3 sccm to 0.8 sccm diluted with nitrogen to achieve a constant concentration of 1% PO. Nonetheless, even in this narrow window the change in conversion PO was quite dramatic, as can be observed in Figure 4.6. In this figure, the conversion data is plotted against the ratio of the catalyst weight, W_{cat}, to the molar flow rate of propylene oxide, F_{co}, a ratio analogous to the residence time for heterogeneous catalysts. The conversion went from 6.3% to 27.4%, a fourfold increase, as the PO flow rate decreased from 0.8 sccm to 0.3 sccm.

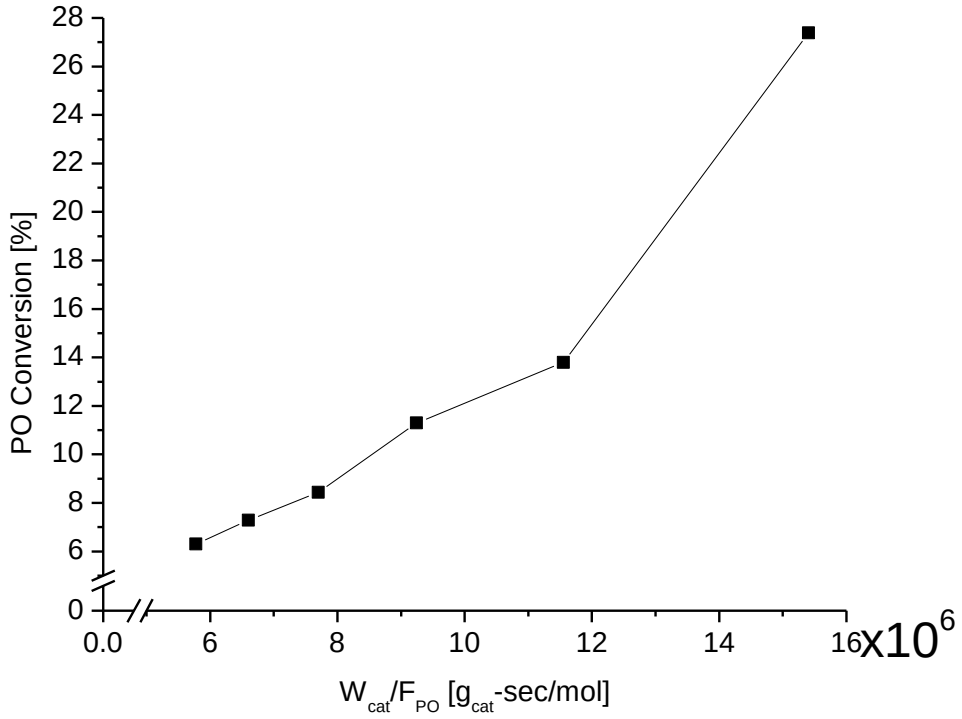

Figure 4.6 Propylene oxide conversion at varying reactant flow rates

The selectivity to the various products of PO decomposition provides information about the mechanism for this reaction. In contrast, acrolein selectivity decreases as the conversion is increased. Following an analysis of the data suggested by literature sources, the data on Figure 4.7 can be used to gain insight on the mechanism of acrolein formation [26]. Note that according to the Delplot technique, a plot of the selectivity vs. conversion can be used to discern whether a reaction product is primary or secondary. Primary species have positive intercepts in such plots whereas non-primary species have a zero intercept. Thus, it can be concluded from Figure 4.7 that the products of PO decomposition are all primary, meaning that all of

them are formed directly from PO through some intermediate. Thus, it cannot be expected that acrolein is formed from the reaction of propanal or allyl alcohol in the surface of the catalyst. Acrolein formation proceeds through a pathway that includes only the oxametallacycle and perhaps some other intermediate.

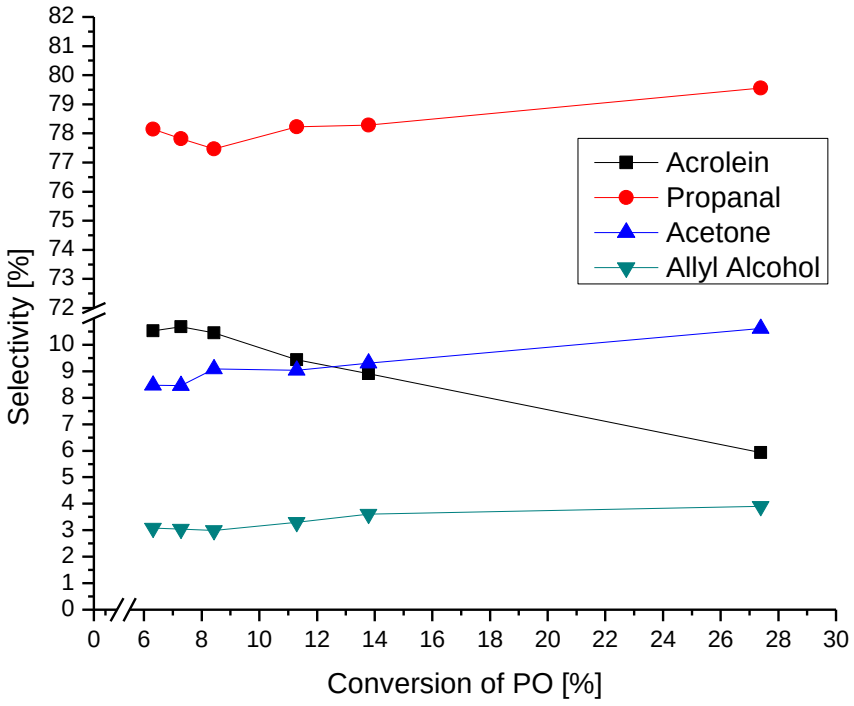

Figure 4.7 Selectivity to various products from PO decomposition in silver. Catalyst running at 267 °C with varying residence time of PO

Another interesting observation from Figure 4.7 is that the selectivity to propanal, acetone and allyl alcohol increased, albeit slightly, with the PO conversion at the same time that the acrolein selectivity decreased. Again, this demonstrates that

acrolein formation is independent of propanal. Moreover, the behavior of this graph gives insight into the relative rates of conversion of each species. Because selectivity to acrolein is lower than for the other products, it can be concluded that this step is also slower than formation of the other products. This makes sense because the formation of acrolein involves dehydrogenation at some point during the reaction pathway, an extra step that propanal or acetone formation does not require.

4.1.3 Effect of Oxygen on the Decomposition of Propylene Oxide

Addition of oxygen to the reaction greatly affects the conversion of propylene oxide into other products. In Figure 4.8, the conversion of PO is plotted under various flows of oxygen to the catalyst. For this experiment, the catalyst was allowed to reach steady state at 267 °C and a flow of 0.5 sccm PO in 50 sccm N_2 while the oxygen flow was adjusted accordingly. Note that, as the O_2/PO feed ratio to the reactor goes from 0, no oxygen, to 2, the conversion of PO doubles from 10.8% to 23% and then levels off fairly quickly at ~26% conversion even as the amount of oxygen is increased to much larger levels than the PO (20:1 ratio). If it can be assumed that these results can be extrapolated to the production of PO from propylene epoxidation, then one can conclude that one quarter of the PO that is produced could end up reacting into other products. This complication may pose an additional problem for the design of a selective catalyst for propylene epoxidation. Even if a given catalyst can prevent the combustion of propylene, it must produce PO selectively and prevent the reaction of PO was well.

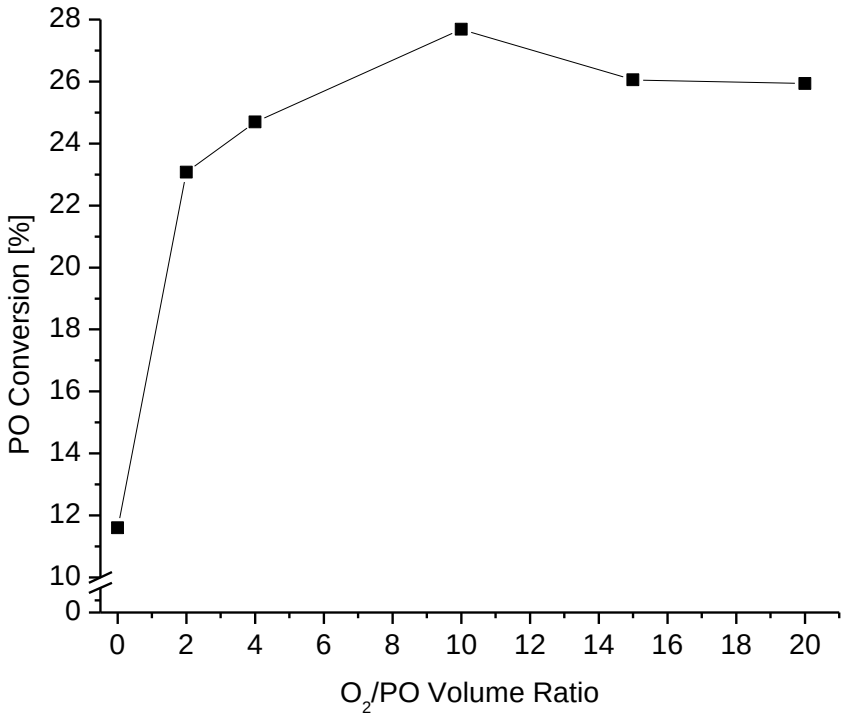

Figure 4.8 Effect of the O_2/PO volume ratio on the conversion of PO. Catalyst running at 267 °C and 0.5 sccm PO

As oxygen is introduced to the reactor, propanal still was the most abundant of the compounds produced from PO isomerization. However, the production of carbon dioxide, CO_2, and other products quickly increased as the feed of O_2 to the reactor was increased with respect to PO, as shown in Figure 4.9. In this figure, the yield of each product was plotted at different values of the O_2/PO volume ratio in the reactor feed.

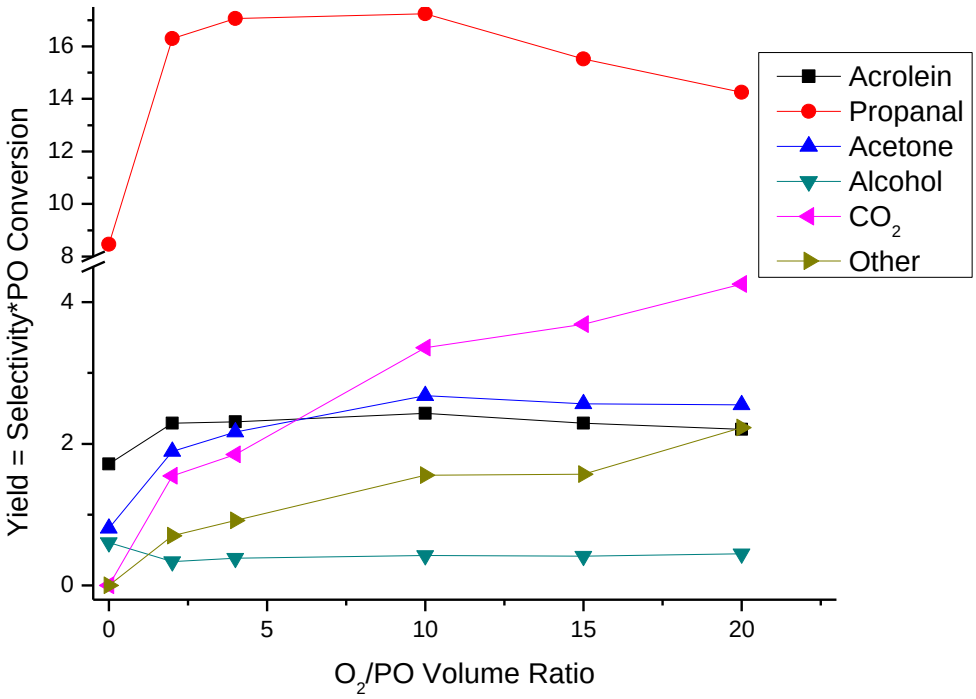

Figure 4.9 Yield to several products at different values of the O_2/PO volume ratio. Catalyst running at 267 °C and 0.5 sccm PO

The reaction products in this experiment were similar to those when no oxygen was included in the reactor, with the only difference being the formation of CO_2 and other products. In this context, the term 'other products' was assigned to peaks in the GC for which the residence time could not be assigned to any compound studied previously, and which based on their retention times likely represent lower molecular weight carbonyl species from the combustion of propanal. The initial increase in PO conversion and yield of the reaction products hints that, whatever the mechanism for PO isomerization is, oxygen does not interfere with it. Instead, oxygen

drives the equilibrium of this reaction to the right through the combustion of the isomerization products.

For propanal, acetone and acrolein, the yield initially increases when oxygen is first introduced to the reactor. Allyl alcohol is the only product for which the yield decreases from 0.6% to 0.3 %. The yield to propanal rapidly increases from 8.5% to 17% and then decreases, while the yield to acetone, acrolein and allyl alcohol remains fairly constant as the O_2/PO ratio increases. At the same time, large amount of carbon dioxide and other products begin to appear. Because at O_2/PO ratios greater than 10 the conversion of PO has reached a constant, the increase in CO_2 production can only be due to the combustion of the isomerization products, specially propanal. Note that these results are similar to those obtained by Lukaski and Barteau for ethylene oxide on Ag(110). Using temperature-programmed desorption, they concluded that oxygen enhanced the formation of oxametallacycle on the silver and that combustion proceeds via oxidation of the acetaldehyde product [27].

4.1.4 Production of Acrolein from Allyl Alcohol

.

The behavior of the allyl alcohol is interesting given that this was the only isomerization product for which the yield decreased as oxygen was introduced to the reactor. A more detailed experiment revealed that in the presence of oxygen, allyl alcohol readily reacts to form acrolein. This experiment was carried by flowing nitrogen through a bubbler containing liquid allyl alcohol. Due to the partial pressure of the liquid, a small amount of the alcohol in the gas phase travels with the nitrogen to the reactor. The results for this experiment are shown in Figure 4.10. Bubbling allyl alcohol to the catalyst at 267 °C, a small portion of the alcohol reacted to form

propanal and acrolein**.** The conversion of the alcohol at these conditions was 4% with no other products detected in the GC. As oxygen was introduced into the reactor, however, most of the allyl alcohol reacted to form acrolein and carbon dioxide. The conversion of the alcohol in the presence of oxygen was 74%, with 80% selectivity to acrolein.

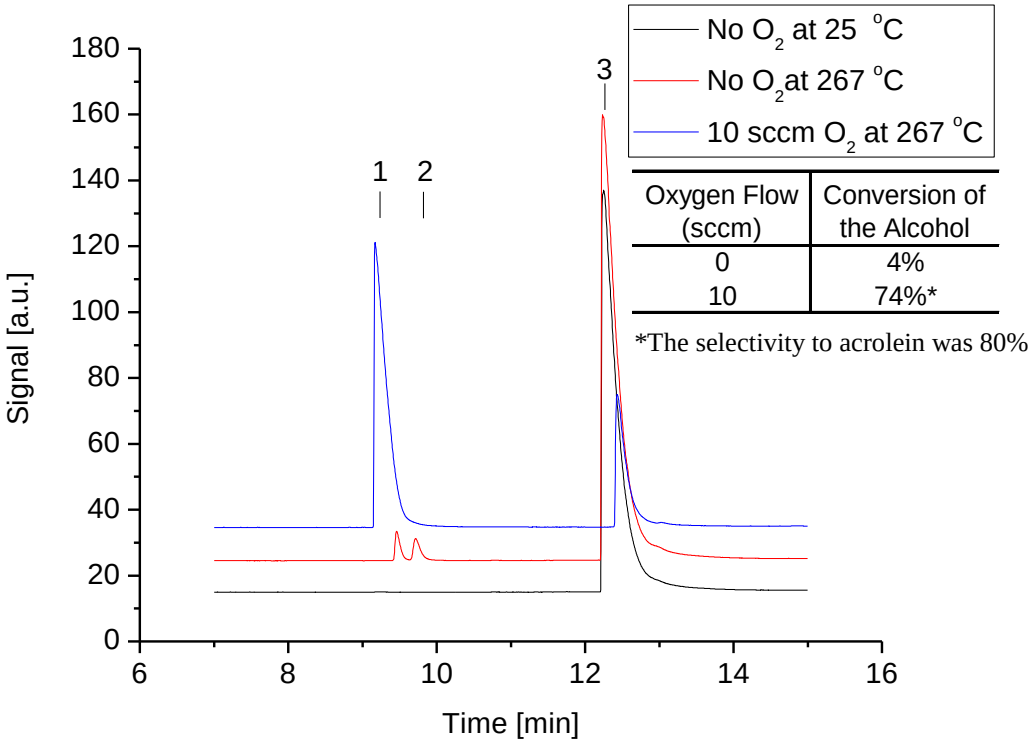

Oxygen Flow (sccm)	Conversion of the Alcohol
0	4%
10	74%*

*The selectivity to acrolein was 80%

Figure 4.10 Facile acrolein formation from allyl alcohol on Ag in the presence of oxygen. The GC spectrum shows the peaks for the products observed (CO_2 peak not included): 1) acrolein, 2) propanal 3) allyl alcohol.

The high conversion of allyl alcohol in the presence of oxygen indicates that even if this compound is formed during propylene epoxidation, it is highly unlikely that it will be detected directly. More importantly, this experiment establishes a pathway for the formation of acrolein. A suggested mechanism for the formation of acrolein from the alcohol could be as follows: oxygen adsorbed on the surface attacks the O-H bond of the alcohol, which subsequently forms an allyl alkoxide on the Ag. The allyl alkoxide dehydrogenates to form acrolein. This mechanism is similar to the one proposed by Brown and Barteau for the reaction of allyl alcohol on the surface of rhodium [29]. But because it was concluded earlier that both acrolein and allyl alcohol were primary products of PO decomposition (section 4.1.4), acrolein formation from PO must proceed through yet another reaction pathway. This pathway is discussed in the following section.

4.2 Proposed Mechanism for the Epoxidation of Propylene

Taking into account all the observations presented in section 4.1, a clear picture of the mechanism of propylene epoxidation begins to emerge. The key link between propylene epoxidation and the decomposition of propylene oxide, shown above, is the assumption that both proceed through an oxametallacycle as an intermediate.

Through the efforts of Barteau and coworkers, it was discovered that the partial oxidation of ethylene occurs through an oxametallacycle [23]. Soon thereafter, it was recognized that an oxametallacycle is the common intermediate for all epoxidation reactions carried on silver. For propylene epoxidation, however, there are two possible configurations of the oxametallacycle; these are shown in Figure 4.11.

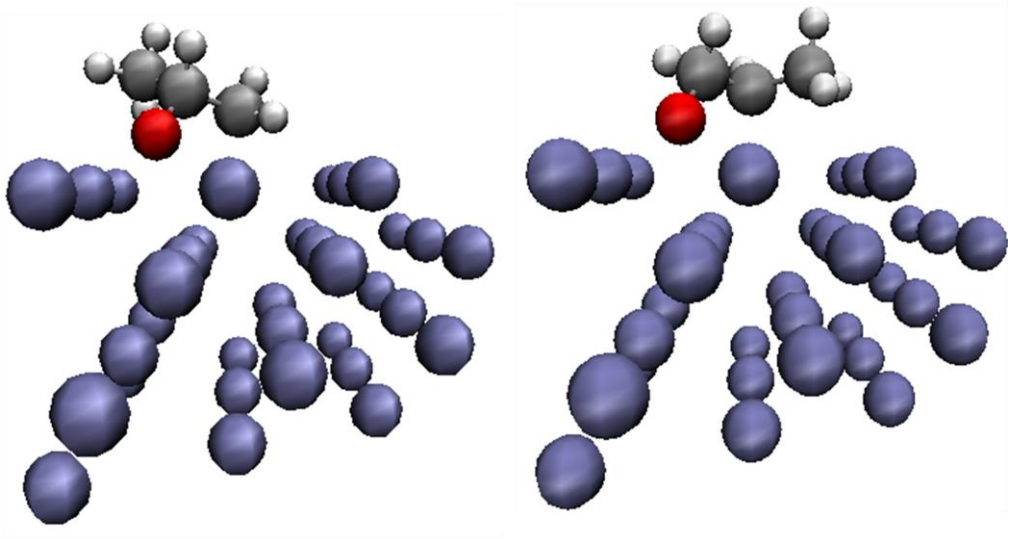

Figure 4.11 Oxametallacycle intermediates for the epoxidation of propylene.

In the OMC1 configuration, the middle carbon carries both the allyl carbon and the oxygen, which in turn is adsorbed to the metal surface. The oxametallacycle in the OMC2 configuration is a straight chain species for which the allyl carbon and the oxygen are bonded to different atoms. Using Density Functional Theory calculations, Medlin, Mavrikakis and Barteau concluded that the OMC1 is slightly more stable, thermodynamically, than the OMC2 [28]. These results were successfully reproduced using the Vienna Ab-Initio Simulation Package (VASP). Thus, it was calculated that the stability of the oxametallacycle is not very different

from the adsorbed PO on the metal surface. Table 4.2 presents the relative energies calculated for the adsorbed PO and the oxametallacycle structures.

Table 4.2 Relative energy calculated for adsorbed PO and the oxametallacycle structures

Species	Relative Energy [kcal/mol] $E_{calc} - E_{PO, ad}$
Adsorbed PO	0
OMC1	-4.6
OMC2	-2.7

Since the adsorbed PO and the oxametallacycle structures are thermodynamically similar, only the activation barrier between the OMC1/2 and adsorbed PO separates each species. Moreover, since OMC1 and OMC2 have similar structures to the products of the isomerization products of PO, it is sensible to assume that acetone and propanal are formed from an oxametallacycle and a subsequent hydrogen shift.

The formation of acrolein and allyl alcohol must proceed through further reaction of the oxametallacycle. According to Brown and Barteau, the oxametallacycle can also undergo dehydrogenation to produce an allyl alkoxide species on the surface of rhodium, see Figure 4.12 [29, 30]. As discussed in section 4.1.4 of this work, the allyl alkoxide may form on silver as well. Extrapolating these results to the observations presented in this work, then it can be concluded that formation of this alkoxide species leads to production of acrolein and allyl alcohol.

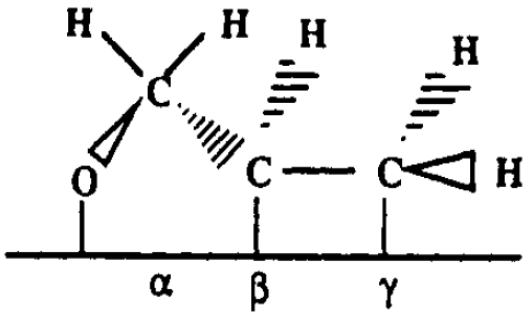

Figure 4.12 Allyl alkoxide (ALK) intermediate for the formation of acrolein and allyl alcohol [29]

Once the oxametallacycle dehydrogenates to form the allyl alkoxide, further reactions give rise to either acrolein or allyl alcohol. If the adsorbed alkoxide species proceeds to a second hydrogen elimination step, then acrolein is formed. In contrast, the alcohol is formed when this alkoxide gains a hydrogen atom to reform the O-H bond. Acrolein formation from allyl alcohol, as shown in Figure 4.10 could also proceed through this allyl alkoxide intermediate. These conclusions are summarized on Figure 4.13, which presents a schematic of the proposed reaction mechanism for the epoxidation of propylene on silver.

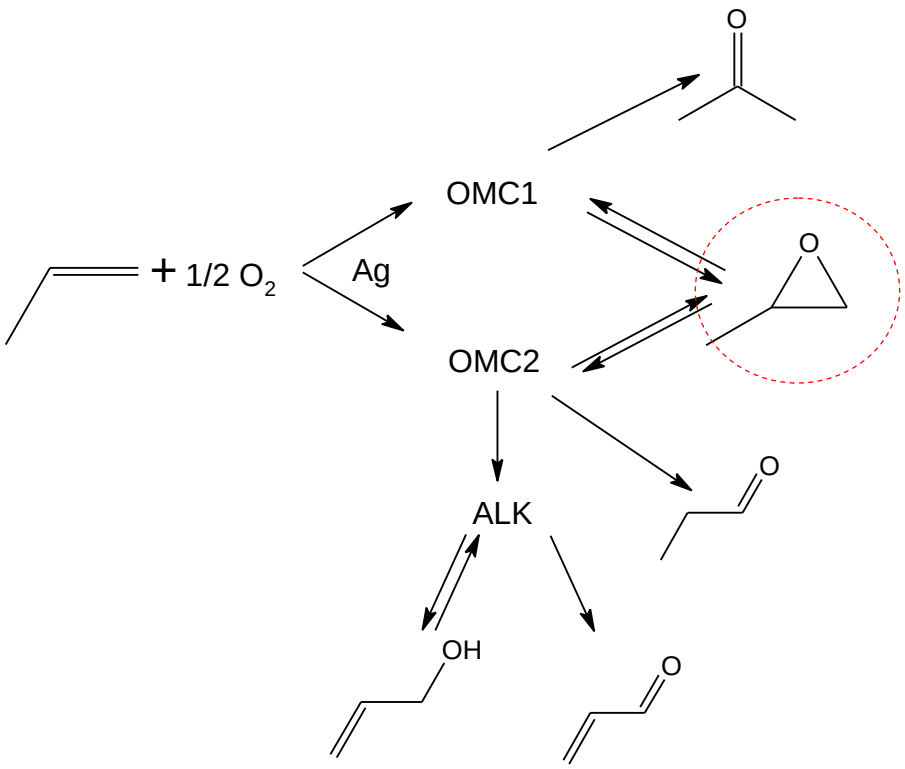

Figure 4.13 Proposed mechanism for the epoxidation of propylene

The proposed mechanism for propylene epoxidation fits the observations discussed in this chapter. However, without a more detailed surface experiment or theoretical tools such as DFT, no more conclusions can be drawn.

Chapter 5

CONCLUSIONS

The production of propylene oxide from the direct epoxidation of propylene has been studied. Several silver-based catalysts have been tested and even though none of them is particularly selective, important kinetic information has been obtained. The dissociation of oxygen on the surface of catalyst appears to be the rate limiting step for propylene oxidation based on the measurements of the apparent activation energy of the reaction and effect of excess propylene in the reactor.

The decomposition of propylene oxide, the desired product from epoxidation, has also been studied in order to gain insight on the mechanism of propylene epoxidation. A mechanism has been proposed that fits well the observations from this experiment. Assuming an oxametallacycle as the intermediate species, it has been concluded that production of acetone, propylene oxide and propanal proceed directly from the oxametallacycle. In addition, literature data shows that the oxametallacycle can further undergo dehydrogenation to produce an allyl alkoxide intermediate. This alkoxide is thought to be the responsible species preceding the formation of allyl alcohol and acrolein.

However, more detailed surface science experiments are needed in order to make further conclusions about the mechanism of epoxidation. The use of computational techniques such as DFT is also needed in order to gain a better understanding of the detailed energies and reaction constants in this mechanism.

REFERENCES

[1] J. P. Dever, K. F. George, W. C. Hoffman, H. Soo, "Ethylene oxide." Kirk-Othmer Encyclopedia of Chemical Technology 5th Ed. (2006): 10, p 632

[2] D. L. Trent, "Propylene oxide." Kirk-Othmer Encyclopedia of Chemical Technology 5th Ed. (2006) 20, p. 720

[3] G. S. Jones, M. Mavrikakis, M. A. Barteau, J. M. Vohs, "First synthesis, experimental and theoretical vibrational spectra of an oxametallacycle on a metal surface" Journal of American Chemical Society 120 (1998) 3196-3204

[4] J. W. Medlin, M. A. Barteau, J. M. Vohs, "Oxametallacycle formation via ring-opening of 1-epoxy-3-butene on Ag(110): a combined experimental/theoretical approach" Journal of Molecular Catalysis A: Chemical 163 (2000) 129-145

[5] S. Linic and M. A. Barteau, "Construction of a reaction coordinate and a microkinetic model for ethylene epoxidation on silver from DFT calculations and surface science experiments" Journal of Catalysis 214 (2003) 200-212

[6] S. Linic, J. T. Jankowiak and M. A. Barteau, "Selectivity driven design of bimetallic ethylene epoxidation catalyst from first principles" Journal of Catalysis 224 (2004) 489-493

[7] J. T. Jankowiak and M. A. Barteau, "Ethylene epoxidation over silver and copper-silver bimetallic catalysts: I. Kinetics and selectivity" Journal of Catalysis 236 (2005) 366-378

[8] "Propylene oxide" Product Overview. Shell Chemicals. Accessed: 30 March 2010 http://www.shell.com/home/content/chemicals/products_services/our_products/propylene_oxide_derivatives/propylene_oxide/product_overview/propylene_oxide_overview.html

[9] J. R. Monnier, "The direct epoxidation of higher olefins using molecular oxygen" Applied Catalysis A General 221 (2001) 73-91

[10] N. W. Cant and W. K. Hall, "Oxidation of labeled olefins over silver" Journal of Catalysis 52 No. 1 (1978) 81-94

[11] Z.-M. Hu, H. Nakai, H. Nakatsuji, "Oxidation mechanism of propylene on an Ag surface: dipped adcluster model study" Surface Science 401 (1998) 371-391

[12] B. Cooker, A.M. Gaffney, J. D. Jewson, A. P. Kahn, W. H. Animus, "Propylene epoxidation using chloride-containing silver catalyst" United States Patent 5780657. Arco Chemical Technology, L. P. (1998)

[13] J. R. Monnier, K. T. Peters and G. W. Hartley, "The selective epoxidation of conjugated olefins containing allylic substituents and epoxidation of propylene in the presence of butadiene" Journal of Catalysis 225 (2004) 374-380

[14] J. C. Dellamorte, J. Lauterbach, M. A. Barteau, "Rhenium promotion of Ag and Cu-Ag bimetallic catalysts for ethylene epoxidation" Catalysis Today 120 (2007) 182-185

[15] J. C. Dellamorte, M. A. Barteau, J. Lauterbach, "Opportunities for catalyst discovery and development: Integrating surface science and theory with high throughput methods" Surface Science 603 (2009) 1770-1775

[16] J. C. Dellamorte, "Investigation of silver based catalysts for ethylene epoxidation: High throughput studies and characterization" (2009) Ph.D. dissertation, University of Delaware.

[17] J. T. Jankowiak, "Epoxide catalysis driven from surface science: application of fundamental studies in surface science and computational chemistry to catalyst design" (2005) Ph.D. dissertation, University of Delaware.

[18] B. K. Bonin and X. E. Verykios, "The oxidation of ethylene over silver-based alloy catalysts. II. Silver-cadmium alloys" Journal of Catalysis 91 (1985) 36-43

[19] R. P. Nielsen and J. H. La Rochelle, "Catalyst for the oxidation of ethylene to ethylene oxide," United StatesPatent 3962136. Shell Oil Company (1975)

[20] Y. Jun, D. Jingfa, Y. Xiaohong and Z. Shi, "Rhenium as a promoter for ethylene epoxidation" Applied Catalysis A 92 (1992) 73-80

[21] X. Liu and C. M. Friend, "Competing epoxidation and allylic hydrogenation activation: trans-β-methylstyrene oxidation on Au(111)" Journal of Physical Chemistry C 114 (2010) 5141-5147

[22] J. K. Norskov, T. Bligaard, A. Loghadottir, S. Bahn, L. B. Hansen, M. Bollinger, H. Bengaard, B. Hammer, Z. Sljivancanin, M. Mavrikakis, Y. Xu, S. Dahl, C. J. H. Jacobsen, "Universality in heterogeneous catalysis" Journal of Catalysis 209 (2002) 275-278

[23] S. Linic and M. A. Barteau, "Formation of a stable surface oxametallacycle that produces ethylene oxide" Journal of the American Chemical Society, 124 (2002) 310-317

[24] NIST Chemistry WebBook, http://webbook.nist.gov/chemistry/ (retrieved May 6, 2010).

[25] Y. Lei, F. Mehmood, S. Lee, J. Greeley, B. Lee, S. Seifert, R. E. Winanas, J. W. Elam, R. J. Meyer, P. C. Redfem, D. Teschner, R. Schlogl, M. J. Pellin, L. A. Curtiss and S. Vajda, "Increased silver activity for direct propylene epoxidation via subnanometer size effects" Science 328 (2010) 224-228.

[26] N. A. Bhore, M. T. Klein, K. B. Bischoff, "The Delplot Technique: A new method for reaction pathway analysis" Industrial and Engineering Chemistry Research 29 (1990) 313-316.

[27] A. C. Lukaski and M. A. Barteau, "Investigation of ethylene oxide on clean and oxygen-covered Ag(110) surfaces" Catalysis Letters 128 (2009) 9-17.

[28] J.W. Medlin, M. Mavrikakis and M. A. Barteau, "Stabilities of substituted oxametallacycle intermediates: implications for regioselectivity of epoxide ring opening and olefin epoxidation" Journal of Physical Chemistry B 130 (1999) 11169-11175

[29] N. F. Brown and M. A. Barteau, "Reactions of unsaturated oxygenates on Rh(111) as probes for multiple coordination of adsorbates," Journal of the American Chemical Society, 114 (1992) 4258-4265.

[30] N. F. Brown and M. A. Barteau, "Reactions of 1-propanol and propionaldehyde on Rh(111)," Langmuir, 8 (1992) 862-869